

INVESTIGATION OF GRAPHENOL AS A NANOFILLER

THESIS

Presented to the Graduate Council of
Texas State University-San Marcos
in Partial Fulfillment
of the Requirements

for the Degree

Master of SCIENCE

by

Brandon G. Henderson, B.S.

San Marcos, Texas
December, 2011

INVESTIGATION OF GRAPHENOL AS A NANOFILLER

Committee Members Approved:

Gary W. Beall, Chair

Clois E. Powell

Luyi Sun

Approved:

J. Michael Willoughby
Dean of the Graduate College

COPYRIGHT

by

Brandon G. Henderson

2011

FAIR USE AND AUTHOR'S PERMISSION STATEMENT

Fair Use

This work is protected by the Copyright Laws of the United States (Public Law 94-553, section 107). Consistent with fair use as defined in the Copyright Laws, brief quotations from this material are allowed with proper acknowledgement. Use of this material for financial gain without the author's express written permission is not allowed.

Duplication Permission

As the copyright holder of the work I, Brandon G. Henderson, authorize duplication of this work, in whole or in part, for educational or scholarly purposes only.

ACKNOWLEDGEMENTS

I would like to thank my family for their patience, love, and support. I want to thank Dr. Gary Beall for his guidance and advice. Thanks are due to my committee members and all the faculty and staff at Texas State University-San Marcos. Many thanks to Maureen Burke, Al Martinez, Tyler Nash, Yelena Nash, Grant Bemis, and all the members of Dr. Beall's research group.

This thesis was submitted on October 14, 2011.

Table of Contents

	Page
ACKNOWLEDGEMENTS	v
LIST OF TABLES	viii
LIST OF FIGURES	ix
CHAPTER	
1 INTRODUCTION AND BACKGROUND	1
1.1 Nanocomposites	1
1.2 Leonardite	2
1.3 Light and Conjugation	3
1.4 Hypothesis.....	4
2 EXPERIMENTAL MATERIALS AND METHODS	5
2.1 Raw Materials and Equipment.....	5
2.2 Preliminary Preparations and Methods.....	6
2.2.1 Reduction of Leonardite	6
2.2.2 Preparation of Graphenol SEM Samples	7
2.2.3 Preparation of Graphenol AFM Samples.....	7
2.2.4 Preparation of Graphenol EDAX Samples	8
2.2.5 Preparation of Leonardite EDAX Sample	8
2.2.6 Preparation of Graphenol Nanocomposite Films.....	8
2.2.7 Preparation of Neat Polyurethane Films	9

2.2.8 Preparation of Clay Nanocomposite Films	9
2.2.9 Preparation of MWCNT Nanocomposite Films	10
2.2.10 Preparation of Optical Microscope Samples.....	10
3 RESULTS AND DISCUSSION	13
3.1 SEM Results.....	13
3.2 EDAX Results.....	13
3.3 AFM Results	14
3.4 TGA Results.....	14
3.5 Tensile Test Results	15
3.6 Optical Microscope Results	17
4 CONCLUSION AND FUTURE RESEARCH.....	56
4.1 Conclusion	56
4.2 Future Research	56
REFERENCES	58

LIST OF TABLES

Table	Page
1. Approximate aspect ratios of graphenol particles as identified in Table 7.....	22
2. Tensile test results for samples 1-3 neat polyurethane specimens.....	42
3. Tensile test results for samples 1-3 graphenol nanocomposite specimens.....	43
4. Tensile test results for sodium cloisite nanocomposite, MWCNT nanocomposite, and neat polyurethane sample 4 specimens	51

LIST OF FIGURES

Figure	Page
1. Dimensions of ASTM D-638 Type IV Specimens.....	11
2. TGA results for Bayhydrol® 124 neat aqueous dispersion	12
3. TGA results for aqueous graphenol suspension.....	12
4. SEM image of leonardite	19
5. SEM image of graphenol	20
6. SEM image of graphenol particles.....	21
7. Identification of graphenol particles used for approximating aspect ratios in Table 1	23
8. EDAX results for leonardite pellet specimen	24
9. EDAX results for graphenol on silicon substrate	25
10. AFM results for graphenol platelet.....	26
11. TGA results for neat polyurethane film sample 1.....	27
12. TGA results for graphenol nanocomposite film sample 1	27
13. TGA results for neat polyurethane film sample 2.....	28
14. TGA results for graphenol nanocomposite film sample 2	28
15. TGA results for neat polyurethane film sample 3.....	29
16. TGA results for graphenol nanocomposite film sample 3	29
17. Tensile test results for neat polyurethane sample 1	30
18. Tensile test results for graphenol nanocomposite sample 1.....	31

19. Tensile test results for neat polyurethane sample 2	32
20. Tensile test results for graphenol nanocomposite sample 2.....	33
21. Tensile test results for neat polyurethane sample 3	34
22. Tensile test results for graphenol nanocomposite sample 3.....	35
23. Tensile test results for neat polyurethane and graphenol nanocomposite sample 1	36
24. Tensile test results for neat polyurethane and graphenol nanocomposite sample 2	37
25. Tensile test results for neat polyurethane and graphenol nanocomposite sample 3	38
26. Tensile test results for neat polyurethane and graphenol nanocomposite sample 1 showing initial slope	39
27. Tensile test results for neat polyurethane and graphenol nanocomposite sample 2 showing initial slope	40
28. Tensile test results for neat polyurethane and graphenol nanocomposite sample 3 showing initial slope	41
29. Tensile test results for neat polyurethane sample 4	44
30. Tensile test results for sodium cloisite nanocomposite film	45
31. Tensile test results for MWCNT nanocomposite film.....	46
32. Tensile test results for neat polyurethane sample 4 and the sodium cloisite nanocomposite	47
33. Tensile test results for neat polyurethane sample 4 and the MWCNT nanocomposite	48
34. Tensile test results for neat polyurethane sample 4 and the sodium cloisite nanocomposite showing initial slope	49

35. Tensile test results for neat polyurethane sample 4 and MWCNT nanocomposite showing initial slope	50
36. Microscope image for nanocomposite sample 1 (20x objective lens).....	52
37. Microscope image for nanocomposite sample 1 (20x objective lens).....	52
38. Microscope image for nanocomposite sample 2 (20x objective lens).....	53
39. Microscope image for nanocomposite sample 2 (20x objective lens).....	53
40. Microscope image for nanocomposite sample 3 (20x objective lens).....	54
41. Microscope image for nanocomposite sample 3 (20x objective lens).....	54
42. Microscope image for MWCNT nanocomposite film (20x objective lens).....	55
43. Microscope image for sodium cloisite nanocomposite film (20x objective lens)	55

1 INTRODUCTION AND BACKGROUND

1.1 Nanocomposites

Polymer nanocomposites are composed of a polymer matrix and a solid particle (filler) that has at least one dimension less than 100 nanometers. There has been growing interest in nanoparticulate fillers for nanocomposites due to significant increases in mechanical, thermal, and electrical properties at low loading levels. Interfacial interaction between matrix and nanofiller leads to significant improvements in various properties of the resulting nanocomposite. When compared to conventional fillers, nanoparticulate fillers can produce orders of magnitude improvement in interfacial interaction between matrix and filler (1). Graphene sheets have been shown to have a Young's modulus of 1.0 ± 0.1 TPa (or roughly $145 \times 10^6 \pm 14.5 \times 10^6$ PSI) (2), intrinsic thermal conductivity of $\sim 5.1 \pm 0.7 \times 10^3$

exfoliation with alkali metals (8), chemical vapor deposition (9), substrate-based thermal decomposition (10), and thermal exfoliation of graphene oxide (11). An inexpensive and readily available source of graphene platelets needs to be identified for the advent of commercialization. It is the focus of this thesis to present the physical properties of cast film nanocomposites made utilizing a new, inexpensive route to functionalized graphene.

1.2 Leonardite

Leonardite is the starting material for functionalizing graphene. It is a low grade coal product that is often a byproduct of near-surface coal seam mining. It is commonly used as a soil conditioner, drilling mud additive, and a binder for taconite iron ore (12). It is composed of fulvic acid, humic acid and humin. Fulvic acid is soluble in alkali, acidic and neutral aqueous solutions. Fulvic acid exhibits a yellow to brown-black color and has the smallest average molecular weight of the three fractions of humic substances with values reported in the range of 175 to 3,570 g/mol. Humic acid is soluble in alkali solutions but insoluble in acidic and neutral solutions. It has a brown to black appearance and a reported average molecular weight range of several hundreds to thousands grams per mole (13). Humin is insoluble in alkali, acidic and aqueous solutions and is believed to be either humic acids that are so intimately bound to mineral matter that they cannot be separated or humic matter of very high carbon content that are therefore insoluble in alkali solution (14). Molecular weights for this fraction have been reported to be well over 1,000,000 g/mol (13).

Leonardite deposits are often found in close proximity to lignite deposits. One theory of the origin of leonardite is that it is the product of lignite oxidation. Another

theory for the origins of leonardite is deposition from the leaching of topsoil by alkaline water and deposited in subsurface strata (15). Leonardite is often referred to as geologic humic matter. It contains very little fulvic acid due to geological processes that have heated and compressed much of the fulvic acid into humic acid (metamorphism). Environmental processes may have also leached out much of the remaining fulvic acid from leonardite (13).

1.3 Light and Conjugation

In order for the human eye to perceive reflected color from a surface, either all colors except for the color perceived are absorbed by the object or only the complementary color is absorbed by the object. For example, the pigment in yellow paint is either absorbing all other wavelengths of visible light corresponding to red, orange, green, blue, and violet or it is only absorbing violet and reflecting all other wavelengths of light. If a surface is perceived by the human eye as white, it must be reflecting all wavelengths of visible light and absorbing none. If it is black, it must be absorbing all wavelengths of visible light and reflecting none (16). Carbon based molecules are capable of absorbing visible wavelengths of light in conjugated systems because the conjugation of pi-pi bonds can lower the band gap of these molecules. When the band gap is close enough, visible light can be absorbed by exciting electrons from the highest occupied molecular orbital into the lowest unoccupied molecular orbital (17).

One of the techniques for producing graphene platelets involves oxidizing graphite. The sheets are exfoliated followed by chemical or thermal reduction (7). The resulting platelets are often referred to as graphene oxide (GO). The aqueous suspensions

are yellow or amber in color (18). Humic acid suspensions derived from leonardite at similar concentrations are black (19). Leonardite, as opposed to GO, must possess an extended conjugate bond system.

1.4 Hypothesis

Our hypothesis is that the humic acid derived from leonardite provides an inexpensive and readily available source of functionalized graphene platelets. Because these suspensions are black in color, we propose that they are highly conjugated and analogues of graphene. They contain carboxylic acid moieties that, as the black color would suggest, do not disturb the conjugation to a major degree and therefore must be primarily located at the edge of the sheet. These carboxylic acid groups, when converted to carboxylate ions by reaction with a base, impart water dispersibility to the particles. We propose investigating using reduced humic acid from leonardite (which we will refer to as graphenol) as a nanocomposite filler.

2 EXPERIMENTAL MATERIALS AND METHODS

2.1 Raw Materials and Equipment

American Colloid Company supplied the Agro-Lig® leonardite and it was used as received. Strem Chemicals, Inc. supplied the Ruthenium, 5% on activated carbon dispersed as a 50% water wet paste (Escat™ 4401). The polyurethane resin, Bayhydrol® 124, was supplied by Bayer MaterialScience, LLC. Cloisite® Na⁺ was refined from montmorillonite clay and was supplied by Southern Clay Products, Inc. The ion exchange resin, Purolite® C100E, was supplied by Purolite® Corporation. MWCNTs, Pyrograf® type PR-19, were provided by Pyrograf® Products, Inc. All other materials and chemicals were purchased from various sources before the creation of this project.

All pH readings were performed using a Corning, Inc. pH Meter 120 with a VWR® symphony® gel epoxy combination pH electrode. Sonication was performed with a Sonics & Materials, Inc. model VC501. Thermogravimetric analysis (TGA) measurements were made using a Thermal Advantage (TA) TGA Q50 with a ramp rate of 20 degrees Celsius per minute from room temperature to 700 degrees Celsius unless otherwise indicated. In all TGA tests, argon was used as a purge gas. The bench top reactor used was a 2 liter (L) model 4522 Parr® reactor. All tensile specimens were cut using an ASTM D-638 Type IV cutting die (dimensions given in figure 1). All tensile tests were performed on a MTS® Sintech™ Model 1D and analyzed with Testworks® version 3.11 software. All scanning electron microscopy (SEM) was performed with a

FEI Company Helios Nanolab™ 400 DualBeam scanning electron microscope. All energy-dispersive X-ray spectroscopy (EDAX) was performed using an EDAX Apollo XL SDD EDS detector. All atomic force microscopy (AFM) was performed using a Veeco Dimension 3100 atomic force microscope and a BudgetSensors® Tap190Al-G cantilever in tapping mode. All visual microscopy was performed using a MicroscopeNet trinocular PLAN phase contrast microscope with an attached 5 MP camera using a 20x objective. Pellets were made using a 7 mm pellet die set from International Crystal Laboratories. The press used to produce pellets and tensile test specimens was a Carver Laboratory Press Model B obtained from Carver, Inc.

2.2 Preliminary Preparations and Methods

2.2.1 Reduction of Leonardite

Three hundred milliliters (ml) of deionized water was added to a 600 ml beaker with 4 grams (gm) of leonardite. The mixture was stirred and the pH adjusted to 12 using a 1 M KOH solution. Deionized water (diH_2O) was added to bring the total volume to 400 ml. The solution was filtered with Whatman grade 1 qualitative filter paper (pore size of 11 micrometers). The resulting dispersion was loaded into the bench top reactor and 3 gm of ruthenium catalyst was added. The reactor was sealed and ultra high purity hydrogen was added until the pressure reached 200 psi. The pressure was slowly released and flushed two more times with hydrogen. The reactor was then pressurized with hydrogen to 520 psi. The temperature of the reactor was then increased from 25° Celsius (C) to 150° C over the course of 30 minutes, with stirring, reaching a pressure of approximately 760 psi. The reactor was allowed to run for 24 hours. The reactor was then cooled followed by a slow release of pressure. The resulting dispersion was filtered

and collected. An ion exchange column with a 3 inch (in) inner diameter and 2 feet (ft) in length was packed with ion exchange beads to a depth of 1 ft. The column was charged with 1 M HCl until the effluent was acidic to pH paper (pH ~ 4). The column was then flushed with diH₂O until the effluent was neutral to pH paper. The suspension was run through the ion exchange column and collected. This procedure was performed three times to produce three batches of graphenol that were used in three polyurethane/graphenol nanocomposite films. Each time the yields were approximately 50%.

2.2.2 Preparation of Graphenol SEM Samples

50 ml of the graphenol solution was filtered using Whatman filter paper with a 0.45 micrometer pore size. The solid left on the filter paper was collected and redispersed into 20 ml diH₂O. A 1 ml syringe was used to collect 1 ml of the graphenol suspension and deposit it on a silicon substrate via spin coating. This step was performed twice in immediate succession. The samples were dried overnight in an oven at 70° C under vacuum (~ 25 mm Hg) prior to SEM testing.

2.2.3 Preparation of Graphenol AFM Samples

The above procedure was duplicated for AFM samples. After filtration, the graphenol suspension was deposited onto a freshly cleaved mica substrate via spin coating. The samples were dried overnight in an oven at 70° C under vacuum (~25 mm Hg) prior to AFM testing.

2.2.4 Preparation of Graphenol EDAX Samples

A silicon substrate target measuring about 1 centimeter (cm) by 1 cm was obtained. About 0.2 ml of graphenol solution was placed on the substrate and allowed to dry. This step was repeated once. The sample was dried overnight in an oven at 70° C under vacuum (~25 mm Hg) prior to EDAX testing.

2.2.5 Preparation of Leonardite EDAX Sample

Approximately 0.12 gm of leonardite was placed in the 7 mm pellet die. The press was used to compress the pellet with an applied load of about 3 metric tons for 15 seconds. The pellet was then dried in an oven at 70° C under vacuum (~25 mm Hg) overnight prior to EDAX testing.

2.2.6 Preparation of Graphenol Nanocomposite Films

A TGA of Bayhydrol® 124 (hereafter referred to as polyurethane) aqueous dispersion (figure 2) determined that it contained approximately 40% by mass polyurethane. A TGA of the graphenol dispersion determined that it was approximately 0.4% by mass graphenol (figure 3). In a 1 liter (L) beaker, 200 gm of the polyurethane suspension was decanted followed by 200 gm of the graphenol suspension. The mixture was sonicated for four minutes. The entire mixture was poured into a 6X10 inch Teflon® coated pan and allowed to dry. After drying (about 7 days), the film was removed from the pan and placed on a glass sheet then placed in a convection oven at 70° C overnight. After the film was removed from the oven, the cutting die and press were used to stamp out specimens for tensile testing. This procedure was performed three times to make three samples of graphenol nanocomposite films.

2.2.7 Preparation of Neat Polyurethane Films

A neat polyurethane film was produced as a control. The above procedure was performed on the neat film sample except where a graphenol suspension was added in the above procedure; exactly the same mass of diH₂O was added instead. This preparation was performed concurrently with the nanocomposite film preparation, the clay nanocomposite film preparation (section 2.2.8), and the MWCNT nanocomposite film preparation (section 2.2.9). When possible, both the nanocomposite and neat polyurethane films were kept under identical conditions (e.g. dried in the oven at the same time).

2.2.8 Preparation of Clay Nanocomposite Film

1.6 gm of Cloisite® Na⁺ (sodium cloisite) was placed in a tared 1 L beaker and diH₂O was added until it reached 200 gm. The mixture was stirred with a magnetic stir bar on a stirring plate for 30 minutes. This mixture was then sonicated for four minutes. This dispersion was cloudy and off white in appearance. In the 1 L beaker, 330 gm of polyurethane suspension and the sodium cloisite dispersion was added. The polyurethane/sodium cloisite aqueous suspension was sonicated for four minutes. The entire mixture was poured into a 6X10 inch Teflon® coated pan and allowed to dry. After drying (about 7 days), the film was removed from the pan and placed on a glass sheet then placed in a convection oven at 70° C overnight. After the film was removed from the oven, a cutting die and press were used to stamp out specimens for tensile

testing. A sample of neat polyurethane was produced concurrently with this sample using the same method but adding only diH₂O where sodium cloisite was added.

2.2.9 Preparation of MWCNT Nanocomposite Film

1.6 gm of MWCNTs were placed in a tared 1 L beaker and diH₂O was added until it reached 200 gm. The mixture was stirred on a stirring plate for 30 minutes. This mixture was then sonicated for four minutes. In the 1 L beaker, 330 gm of polyurethane suspension and the MWCNT dispersion was added. The polyurethane/MWCNT aqueous suspension was sonicated for four minutes. The entire mixture was poured into a 6X10 inch Teflon® coated pan and allowed to dry. After drying (about 7 days), the film was removed from the pan and placed on a glass sheet then placed in a convection oven at 70° C overnight. After the film was removed from the oven, a cutting die and press were used to stamp out specimens for tensile testing. A sample of neat polyurethane was produced concurrently with this sample using the same method but adding only diH₂O where MWCNT was added.

2.2.10 Preparation of Optical Microscope Samples

All film samples for optical microscopy were prepared by cutting a square measuring about 1 cm by 1 cm from each film. Each film square was then cleaved, from one corner to the opposite corner, with a razor blade at an approximately 45° angle. The specimen was then placed on a glass microscope slide and the thinnest portion of the film examined using a 20x objective lens.

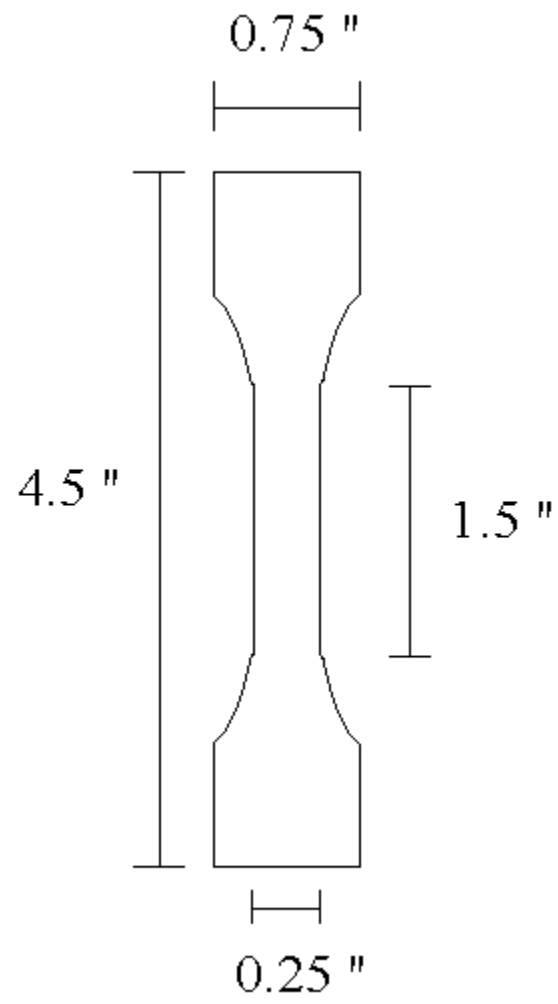


Figure 1. Dimensions of ASTM D-638 Type IV Specimens.

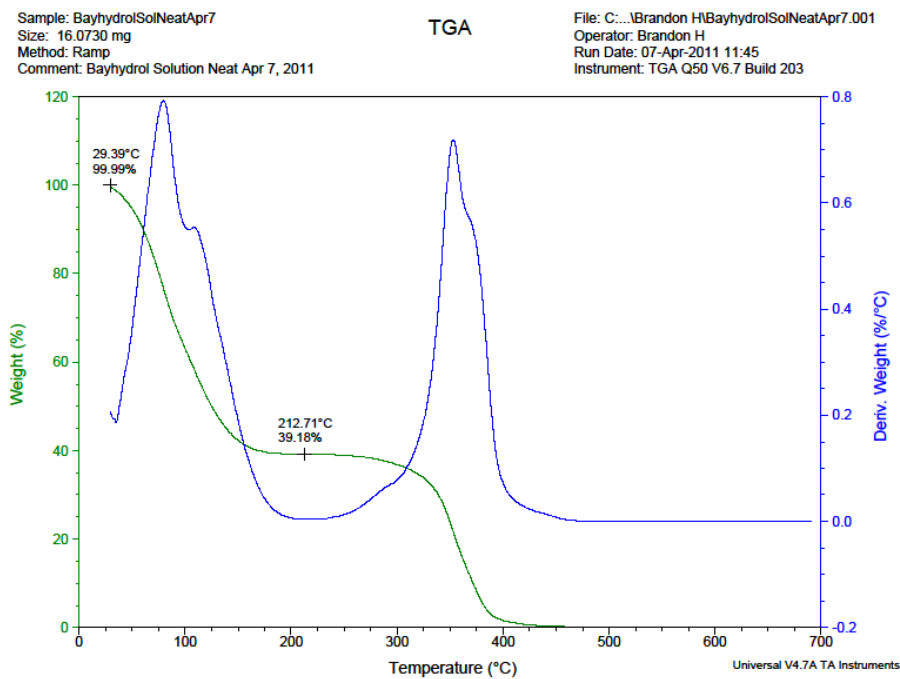


Figure 2. TGA results for Bayhydrol® 124 neat aqueous dispersion.

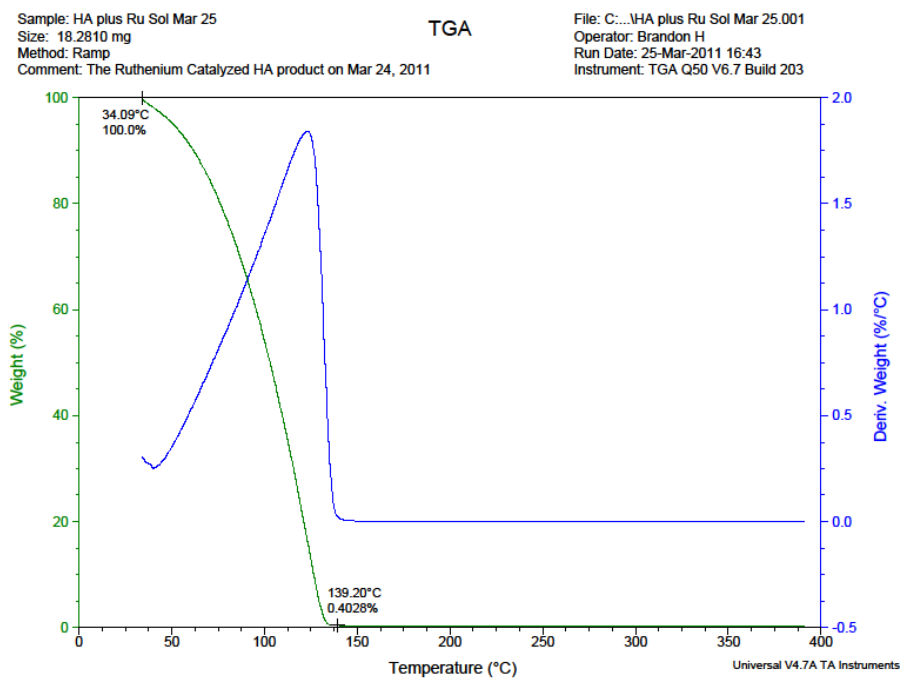


Figure 3. TGA results for aqueous graphenol suspension.

3 RESULTS AND DISCUSSION

3.1 SEM Results

An SEM analysis was conducted on spin coated specimens of both leonardite (figure 4) and graphenol (figure 5) showing a sheet-like morphology and lateral dimensions in the range of 400-550 nanometers. Additional SEM images of graphenol show a lateral dimension range of approximately 115-550 nanometers (figure 6). An approximation of the aspect ratios with regard to width and length is given in table 1 and ranges from 274:1 to 1310:1. The approximations are made for graphenol particles shown in figure 7 and assume a thickness of 0.42 nm determined from the AFM results in section 3.3.

3.2 EDAX Results

An EDAX was performed on a leonardite pellet to determine the carbon to oxygen content ratio of the pellet. As demonstrated in figure 8, the atomic ratio of carbon to oxygen is over 93:7. An EDAX was performed on graphenol with a silicon substrate (figure 9). The atomic ratio of carbon to oxygen in this sample is around 97:3. If all oxygen containing functional groups on a leonardite sheet are carboxylic acids the reduction of leonardite (section 2.2.1) would increase the carbon to oxygen ratio by a factor of 2. The carbon to oxygen ratio increases from about 14:1 in leonardite to about 32:1 in graphenol which is an increase of a factor of about 2.3. The thickness of the

graphenol specimen was not enough to completely mask any contribution of the silicon substrate in this experiment. This is evidenced by the peak corresponding to the $K\alpha$ energy of silicon at about 1.74 keV. Silicon wafers are known to contain oxygen (21) and this may be the cause of the higher than expected carbon to oxygen ratio.

3.3 AFM Results

The graphenol particles were tested using AFM to determine the thickness of a single particle. The average thickness (R_z) of the graphenol sheet shown in figure 10 is 0.42 nanometers which is in close agreement with published reports of the thickness of single graphene sheets of around 0.4 nanometers (6). The size of the graphenol sheet shown in figure 10 is in the range of 2.5 by 1.5 micrometers and the anisotropic aspect ratio with regard to width is then about 3571:1 and with regard to length is about 5952:1.

3.4 TGA Results

TGA was performed on each of the three neat polyurethane samples and the three graphenol nanocomposite samples. In the first sample, the neat polyurethane film left a residue of 0.1945% when the temperature reached approximately 500° C (figure 11). TGA of the concurrently made graphenol nanocomposite film was also run to determine the weight percent loading of graphenol in polyurethane. As shown in figure 12, the graphenol nanocomposite film left a residue of 1.397% at approximately 500° C leading to the conclusion that the first graphenol nanocomposite film was loaded at about 1.2% by weight. This procedure was repeated on the second neat film sample (figure 13) and the second graphenol nanocomposite film sample (figure 14). The second neat film sample left a residue of 0.2112% at about 500° C and the second graphenol

nanocomposite film left a residue of 1.380% which indicates it was loaded at about 1.17% by weight. In the third film sample, the TGA shows the residue left at approximately 500° C is 0.1186% in the neat sample (figure 15) and 1.471% (figure 16) in the graphenol nanocomposite sample which indicates it has a loading of about 1.35% by weight.

3.5 Tensile Test Results

Three samples of neat polyurethane and graphenol nanocomposite films were concurrently produced and used for tensile testing. The results of the specimens from neat polyurethane sample 1 are shown in figure 17 and graphenol nanocomposite sample 1 in figure 18. Sample 2 neat polyurethane and graphenol nanocomposite are shown in figures 19 and 20 respectively. Neat polyurethane sample 3 tensile test results are shown in figure 21 and graphenol nanocomposite sample 3 in figure 22. In order to compare these results, a graph with the neat polyurethane in blue and the graphenol nanocomposite in red is presented for sample 1 (figure 23), sample 2 (figure 24), and sample 3 (figure 25). The only sample where there is an obvious difference is sample 1 where the slope of the load/% elongation line is much higher in the graphenol nanocomposite as compared to the neat polyurethane. A closer view is given for sample 1 (figure 26), sample 2 (figure 27), and sample 3 (figure 28) to compare initial slopes. Young's modulus was calculated for all samples and the results for the neat polyurethane samples are given in table 2; the results for the graphenol nanocomposite samples are given in table 3. In graphenol nanocomposite sample 1, the average Young's modulus increased by over 250%. The Young's modulus for sample 2 decreased in the graphenol nanocomposite compared to the polyurethane sample by about 33% and stayed about the same in sample

3. The peak load on specimens 1 and 2 of graphenol nanocomposite sample 1 is not the point at which they yielded, but the maximum load of the load cell used. Specimen 4 of graphenol nanocomposite sample 1 has a thickness much lower than the other specimens of that sample and reached a peak load of only 22.50 pounds before yielding.

Tensile testing was performed on specimens from a concurrently produced neat polyurethane film, MWCNT nanocomposite film (loaded at 1.2% by weight) and sodium cloisite nanocomposite film (loaded at 1.2% by weight). The results for the neat polyurethane film sample 4 specimens are given in figure 29, for the sodium cloisite nanocomposite film specimens in figure 30, and for the MWCNT nanocomposite film specimens in figure 31. The tensile test results comparing sodium cloisite and the neat polyurethane samples are given in figure 32. The tensile test results comparing MWCNT and neat polyurethane samples are given in figure 33. A closer view comparing the initial slopes of sodium cloisite and neat polyurethane specimens is given in figure 34. A closer view comparing the initial slopes of MWCNT and neat polyurethane specimens is given in figure 35. Young's modulus was calculated for all three of these samples and the results are given in table 4. There was a slight increase (about 7%) in Young's modulus for the sodium cloisite nanocomposite compared to the neat polyurethane specimens. There was an increase in Young's modulus of the MWCNT specimens of about 16% compared to the neat polyurethane specimens. Both the sodium cloisite and MWCNT specimens show an increase in Young's modulus but the magnitude is smaller than the increase shown in graphenol nanocomposite sample 1 (~250%) at similar loadings.

The tensile test results between specimens from the four neat polyurethane films show a large variation (about 50%) in the Young's modulus. This was unexpected and it is unclear why this occurred.

3.6 Optical Microscope Results

To understand why there was an increase in Young's modulus for graphenol nanocomposite sample 1, a decrease in sample 2 and very little change in sample 3, the three samples were inspected visually. It was observed that sample 1 had a much smoother texture than sample 2 and sample 3. The samples were then examined via optical microscopy. The results from graphenol nanocomposite sample 1 are given in figures 36 and 37. The results from graphenol nanocomposite sample 2 are shown in figures 38 and 39. The results from graphenol nanocomposite sample 3 are shown in figures 40 and 41. If the nanofiller in the nanocomposites was well dispersed then optical examination would be optically clear. None of the graphenol nanocomposite film samples were optically clear. There was some agglomeration in graphenol nanocomposite film sample 1 and larger agglomerates observed in graphenol nanocomposite samples 2 and 3. While the dispersion in sample 1 was not ideal, it was certainly better than the dispersion in samples 2 and 3. The graphenol suspensions were filtered before inclusion in the nanocomposites (section 2.2.1). Therefore, these are not very large particles but instead are agglomerates that have been included in the nanocomposite films. Graphenol nanocomposite sample 1 shows the most increase in Young's modulus and also has a comparatively low level of agglomeration. Graphenol nanocomposite samples 2 and 3 have no change or a reduction in Young's modulus and have a comparatively high level of agglomeration. These agglomerates act as stress

concentrators and lower the tensile modulus and strength. It is unclear whether these agglomerates are forming in the graphenol suspension after filtration or during the film casting process but they have a dramatic affect on the Young's modulus of the samples. Optical microscopy was performed on the sodium cloisite nanocomposite film (figure 42) and the MWCNT nanocomposite film (figure 43). The sodium cloisite and MWCNT nanocomposite films both appeared optically clear. The MWCNT nanocomposite film showed striations from the razor blade cleavage but a comparatively low level of agglomeration. The sodium cloisite and MWCNT nanocomposite films are relatively well dispersed when compared to the graphenol nanocomposite films.

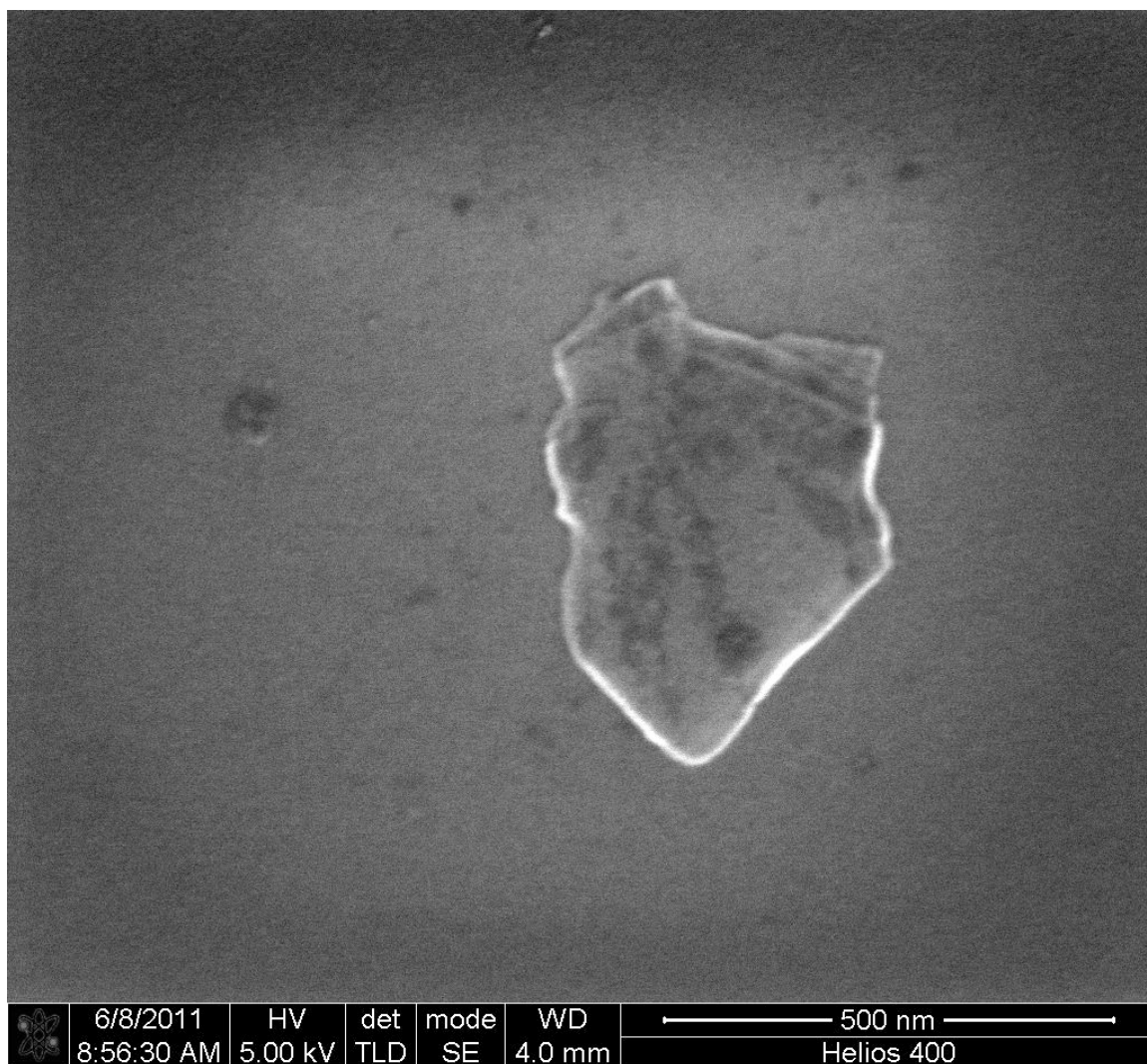


Figure 4. SEM image of leonardite.

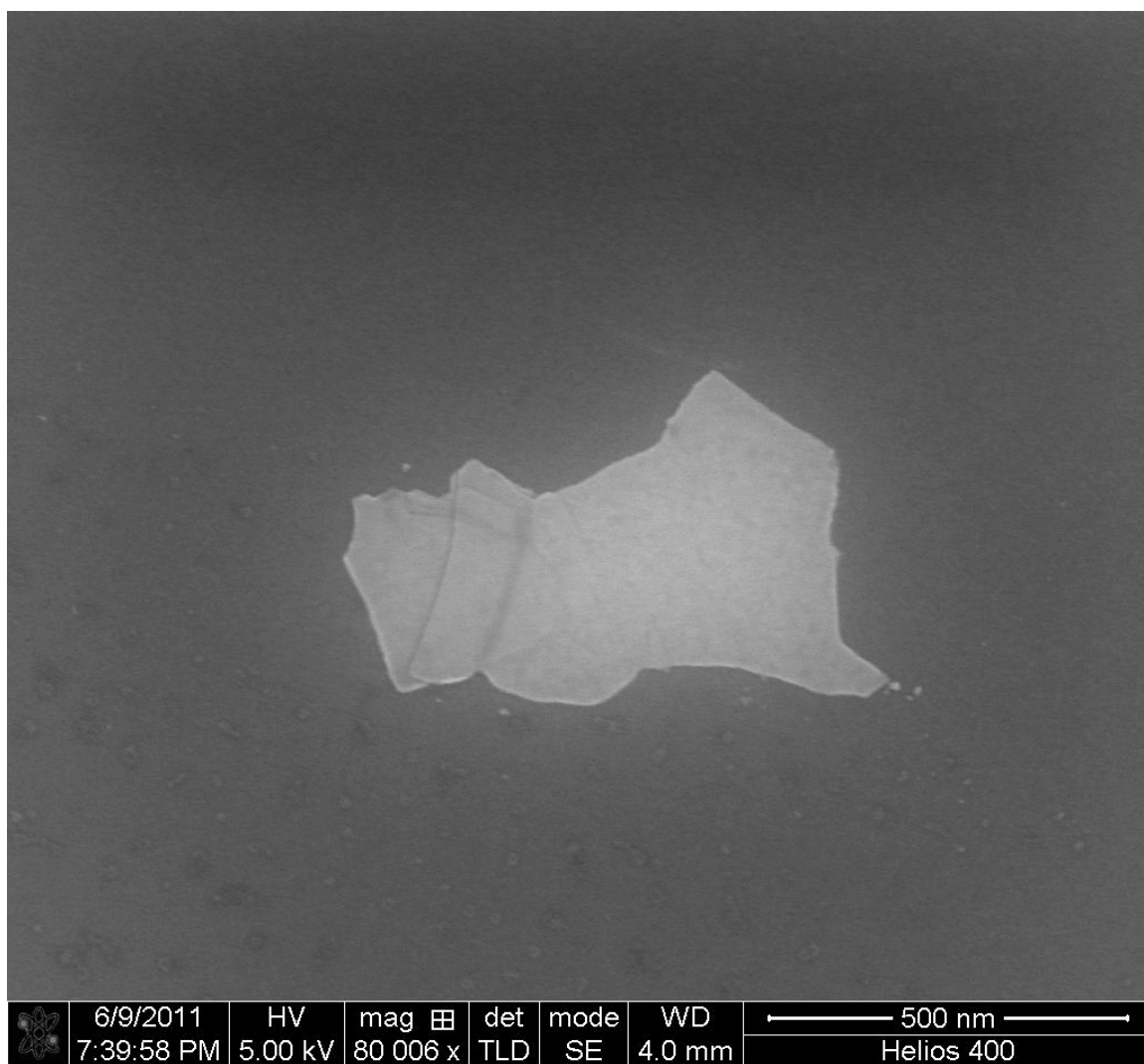


Figure 5. SEM image of graphenol.

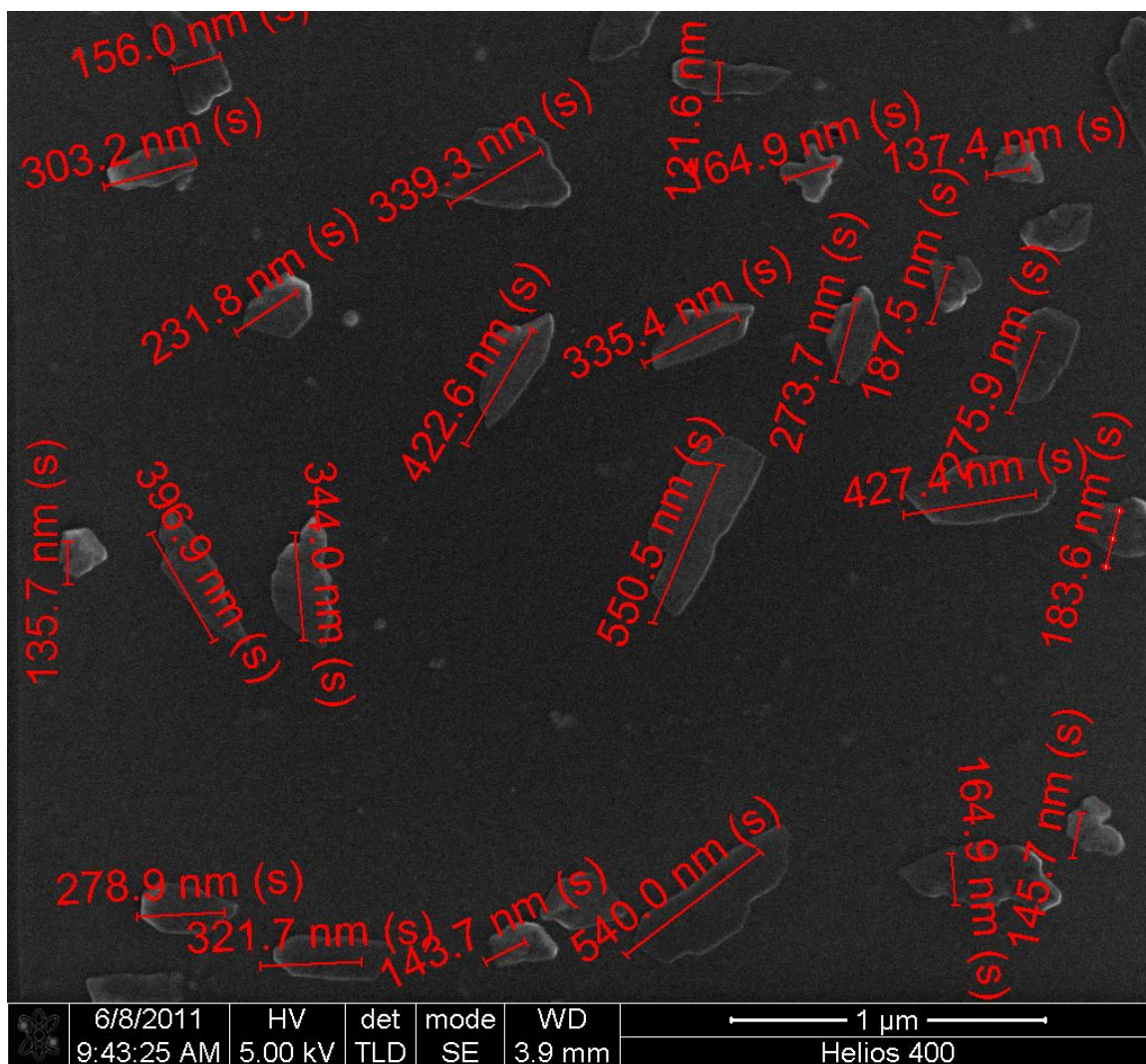


Figure 6. SEM image of graphene particles.

Table 1. Approximate aspect ratios of graphenol particles as identified in Table 7.

Graphenol Particle Number	Width (nm)	Length (nm)	Thickness (nm)	Anisotropic Aspect ratio (Width)	Anisotropic Aspect ratio (Length)
1	156	420	0.4	390	1050
2	150	303	0.4	375	757.5
3	200	231	0.4	500	577.5
4	240	339	0.4	600	847.5
5	121	340	0.4	302.5	850
6	165	165	0.4	412.5	412.5
7	137	137	0.4	342.5	342.5
8	165	422	0.4	412.5	1055
9	150	335	0.4	375	837.5
10	160	273	0.4	400	682.5
11	160	187	0.4	400	467.5
12	158	276	0.4	395	690
13	185	427	0.4	462.5	1067.5
14	115	183	0.4	287.5	457.5
15	186	550	0.4	465	1375
16	170	344	0.4	425	860
17	130	397	0.4	325	992.5
18	136	136	0.4	340	340
19	162	279	0.4	405	697.5
20	137	322	0.4	342.5	805
21	139	144	0.4	347.5	360
22	192	540	0.4	480	1350
23	165	435	0.4	412.5	1087.5
24	146	182	0.4	365	455

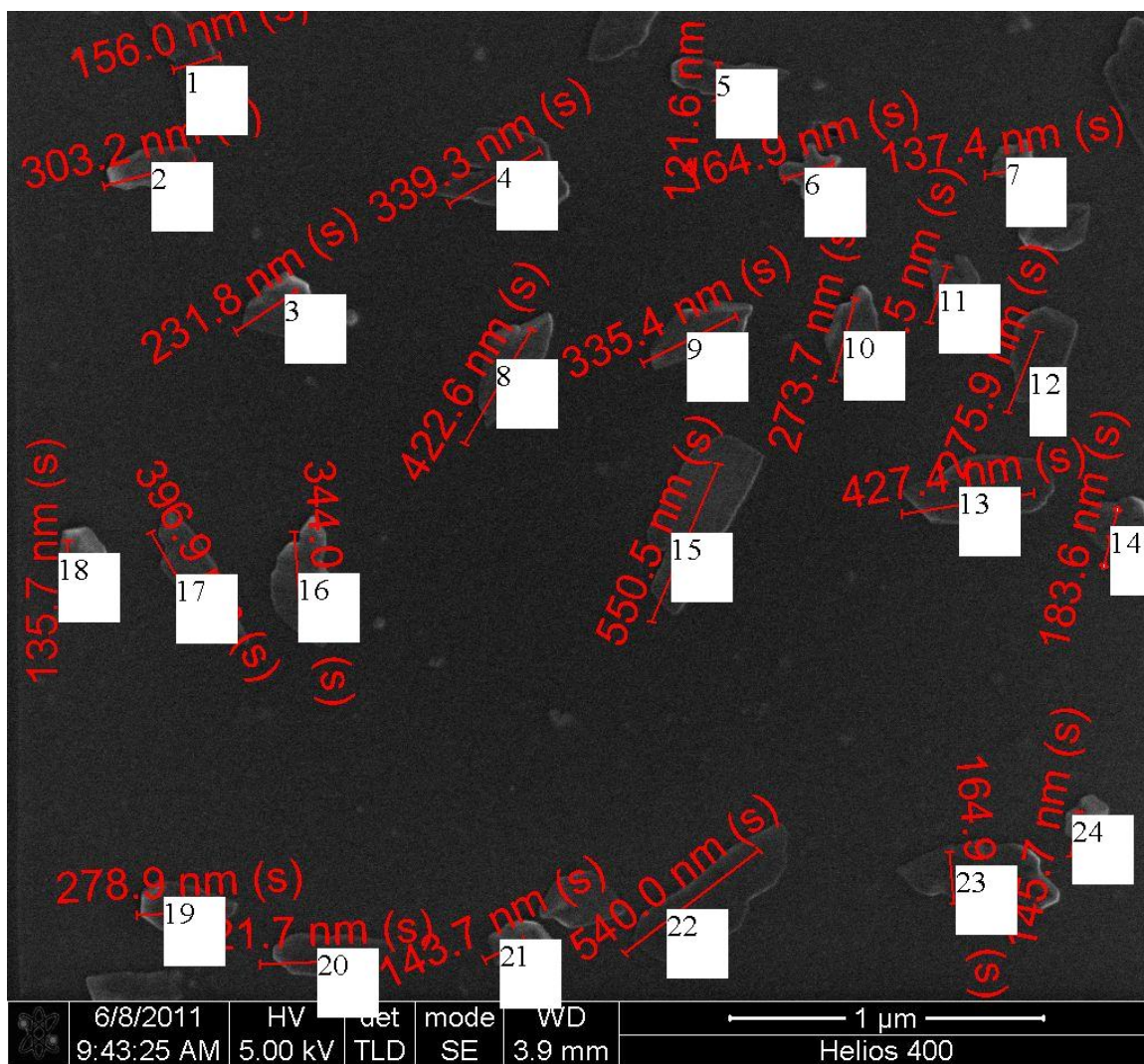
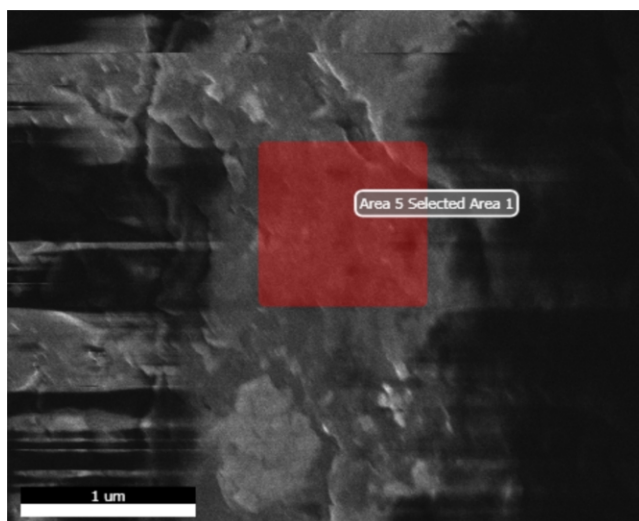


Figure 7. Identification of graphene particles used for approximating aspect ratios in Table 1.

EDAX TEAM EDS

Sample Name: Leonardite

Area 5



Selected Area 1

Det 1

kV: 10

Mag:69896

Takeoff:35

Live Time:1000

Amp Time:12.8

Resolution:130.2

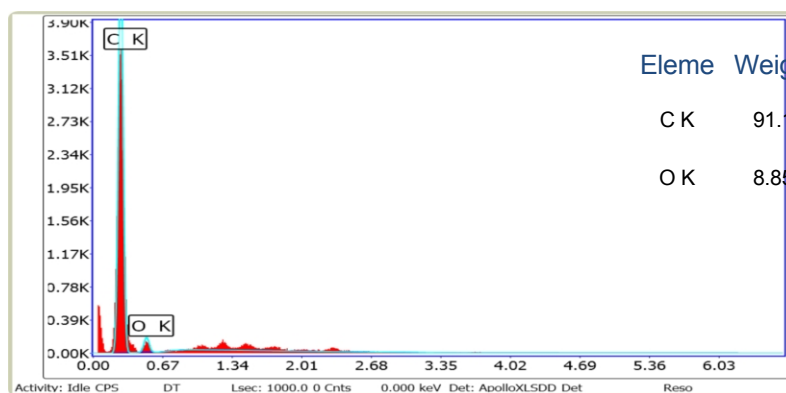
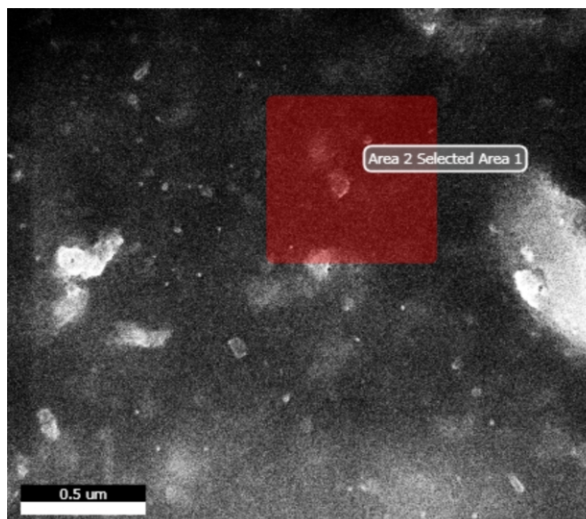


Figure 8. EDAX results for leonardite pellet specimen.

EDAX TEAM EDS

Sample Name: Graphenol

Area 2



Selected Area 1

Det 1

kV: 5

Mag:100017

Takeoff:35

Live Time:1000

Amp Time:12.8

Resolution:130.2

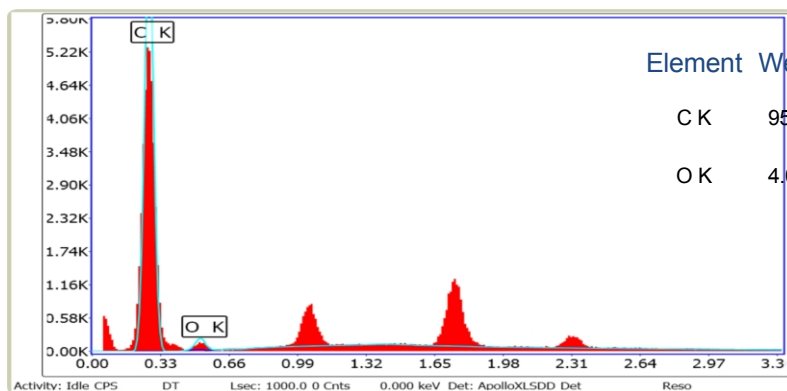


Figure 9. EDAX results for graphenol on silicon substrate.

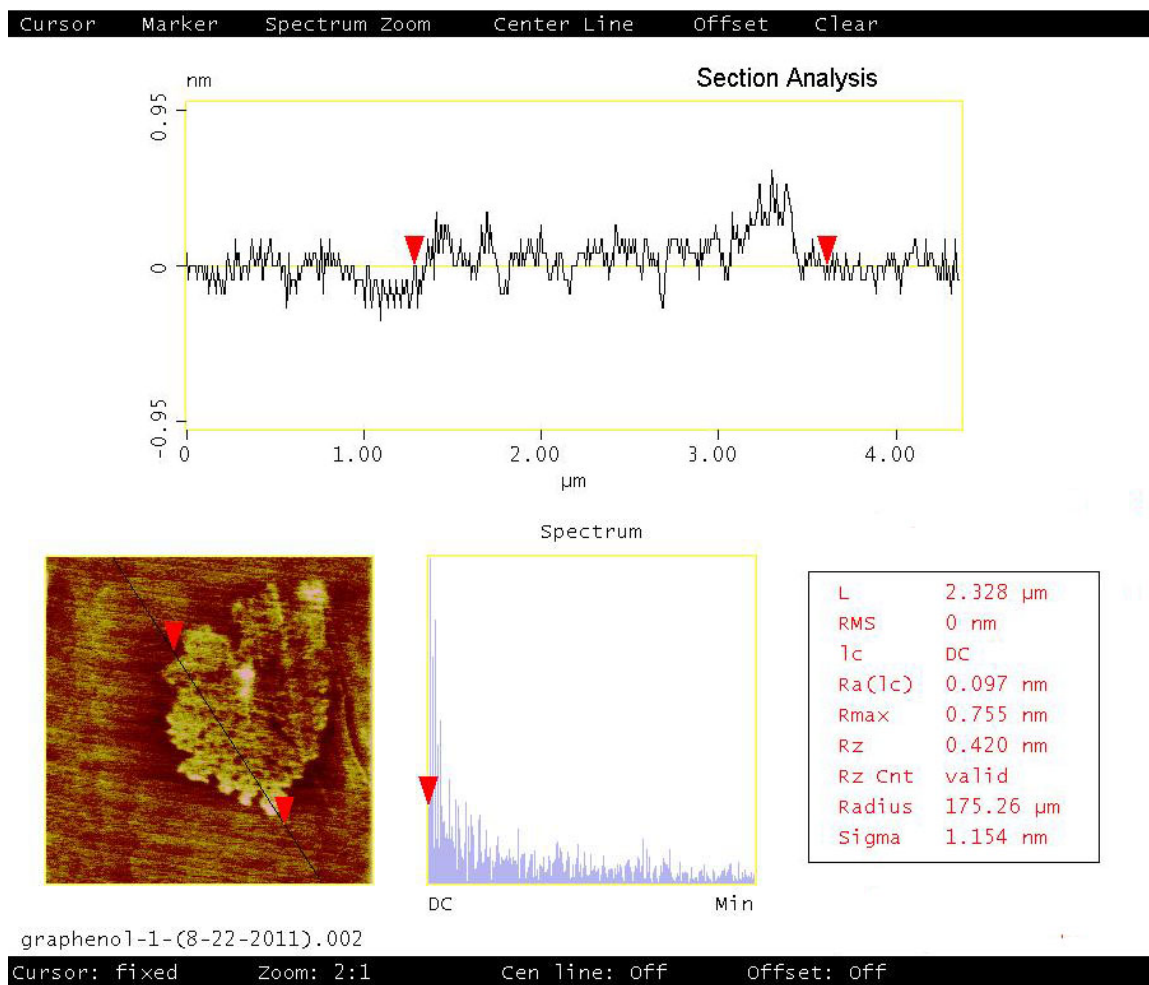


Figure 10. AFM results for graphene platelet.

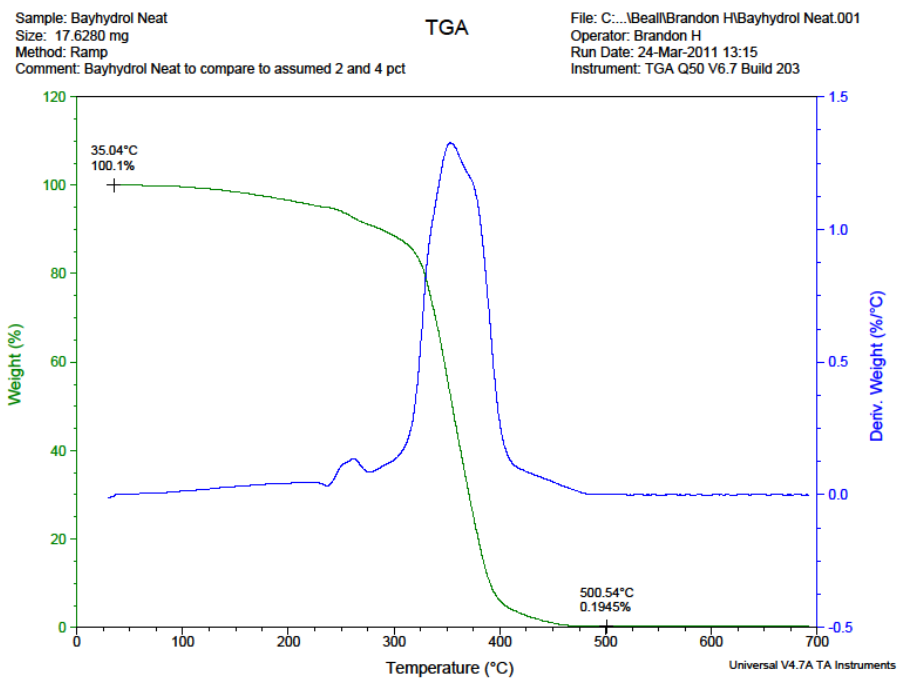


Figure 11. TGA results for neat polyurethane film sample 1.

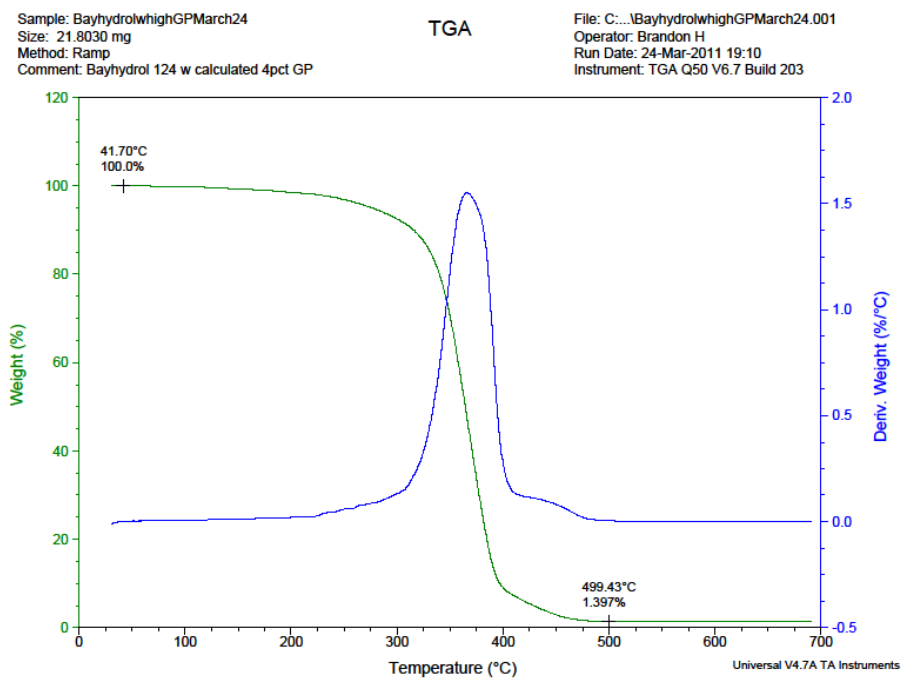


Figure 12. TGA results for graphene nanocomposite film sample 1.

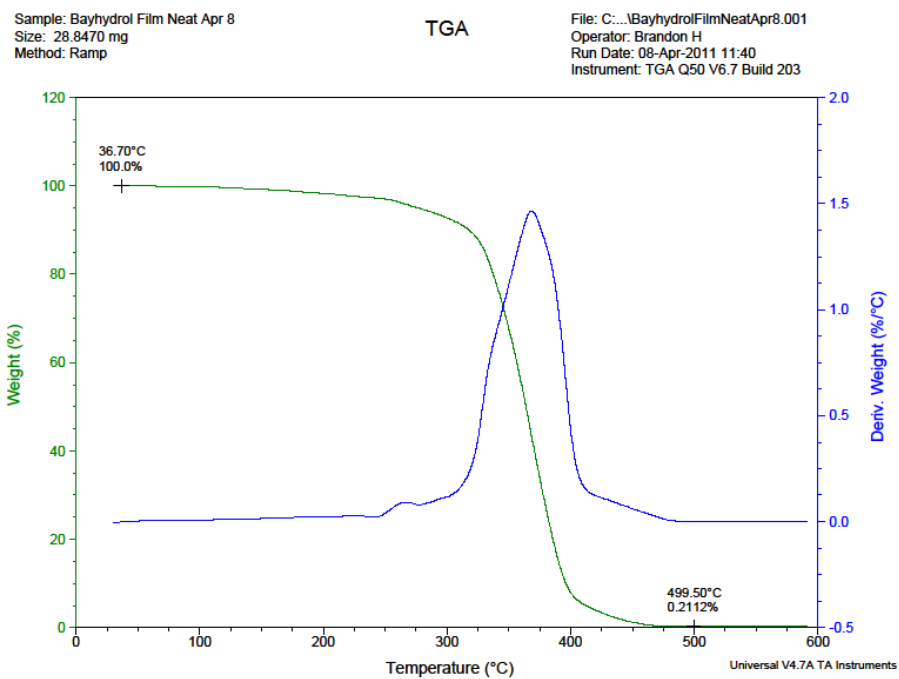


Figure 13. TGA results for neat polyurethane film sample 2.

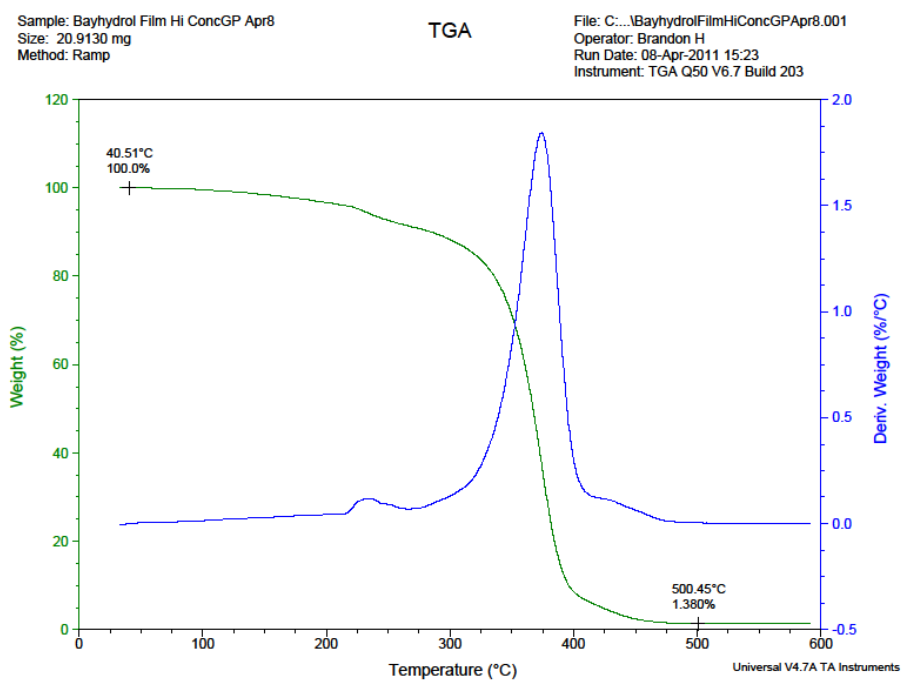


Figure 14. TGA results for graphenol nanocomposite film sample 2.

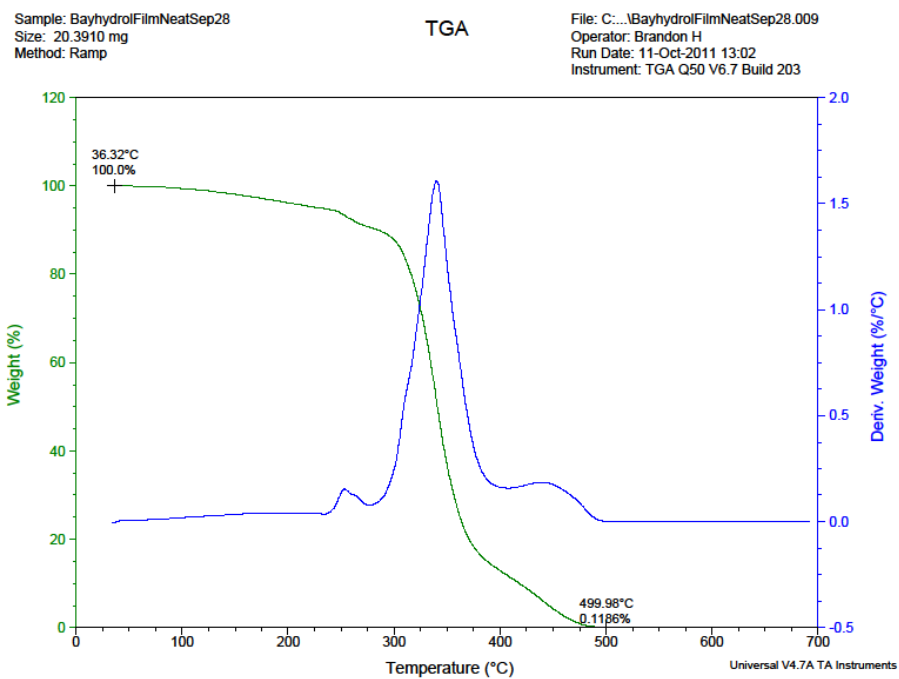


Figure 15. TGA results for neat polyurethane film sample 3.

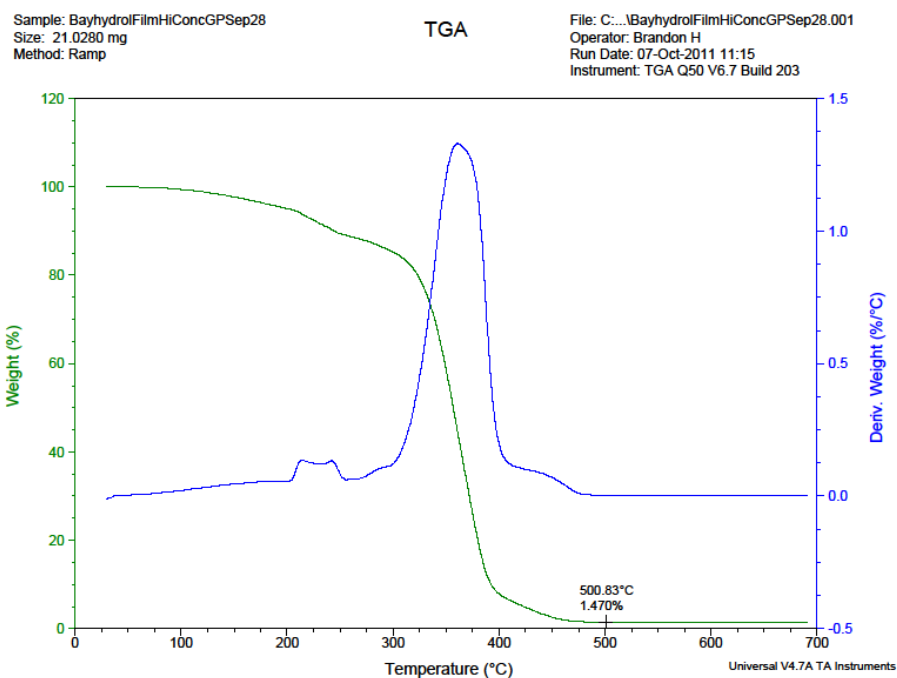


Figure 16. TGA results for graphene nanocomposite film sample 3.

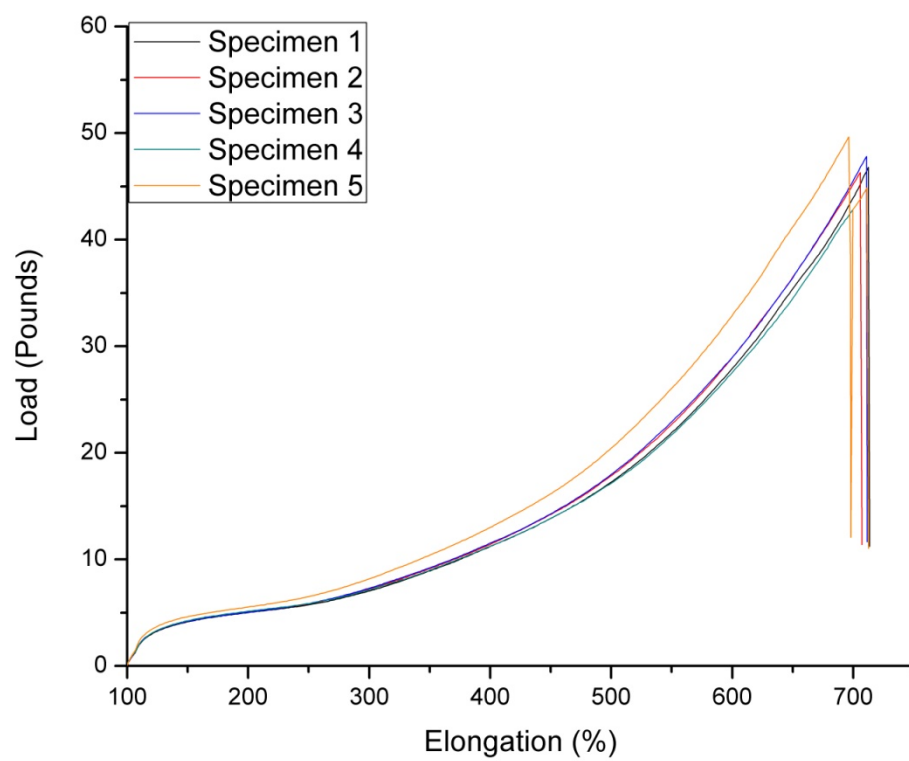


Figure 17. Tensile test results for neat polyurethane sample 1.

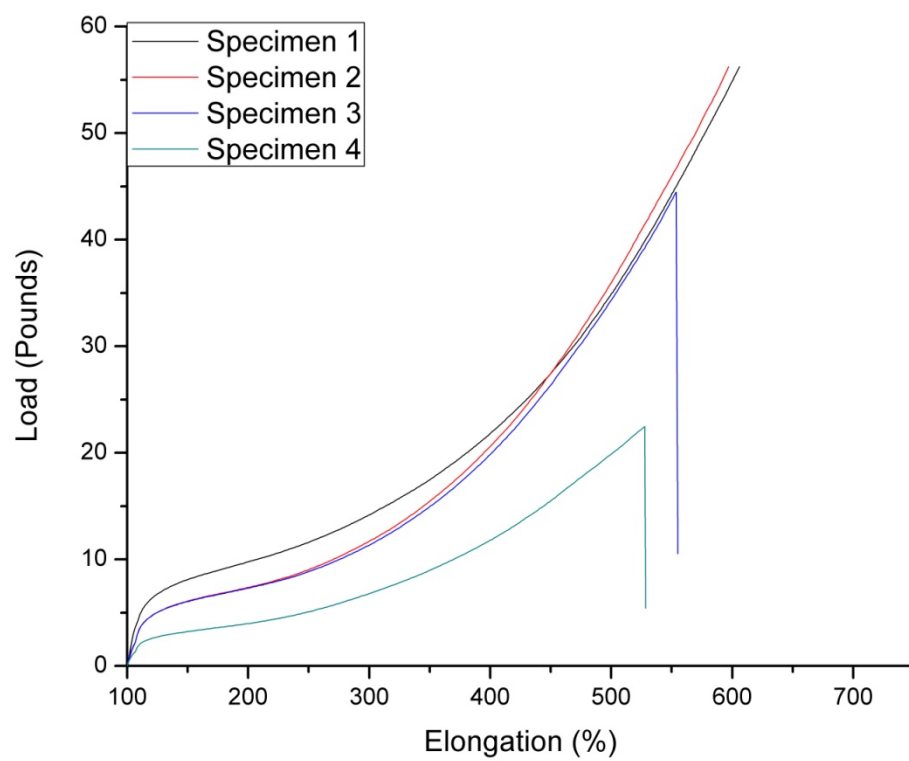


Figure 18. Tensile test results for graphenol nanocomposite sample 1.

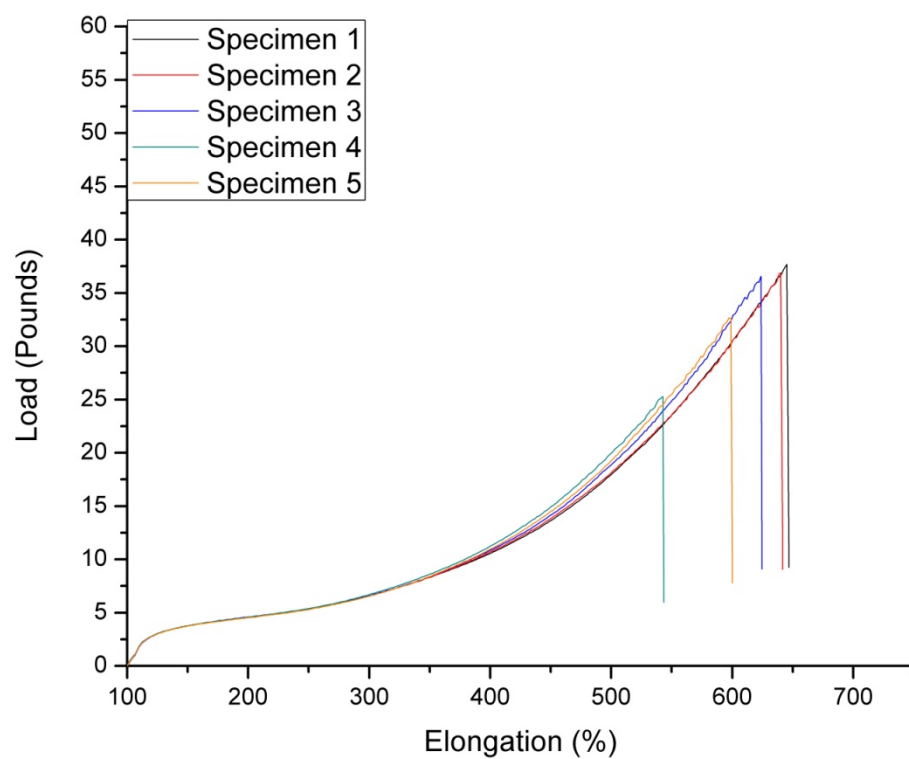


Figure 19. Tensile test results for neat polyurethane sample 2.

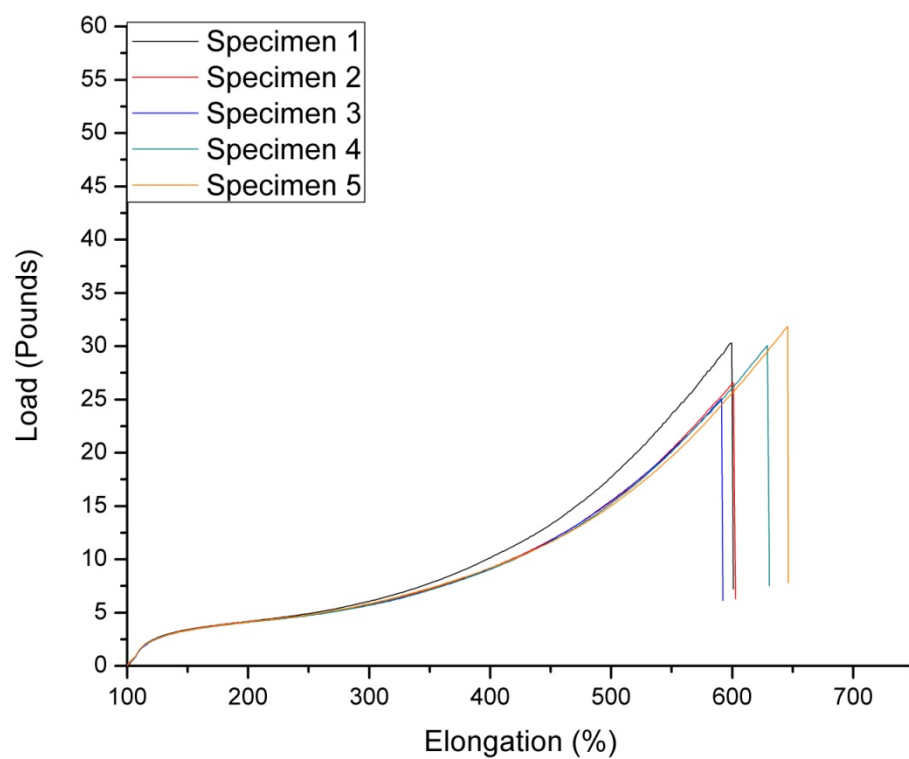


Figure 20. Tensile test results for graphene nanocomposite sample 2.

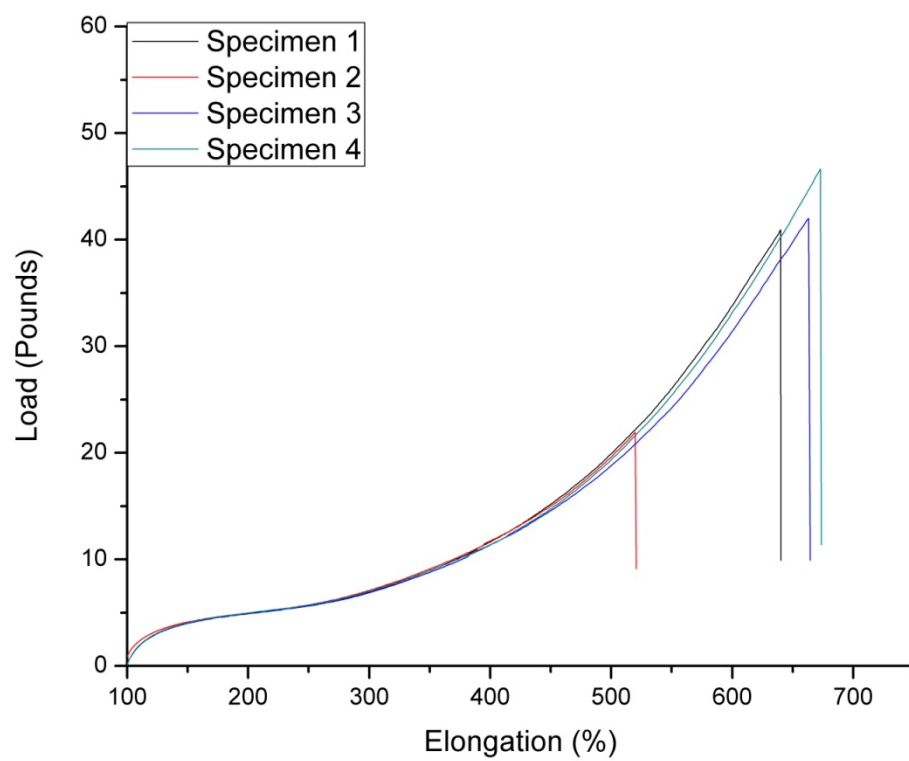


Figure 21. Tensile test results for neat polyurethane sample 3.

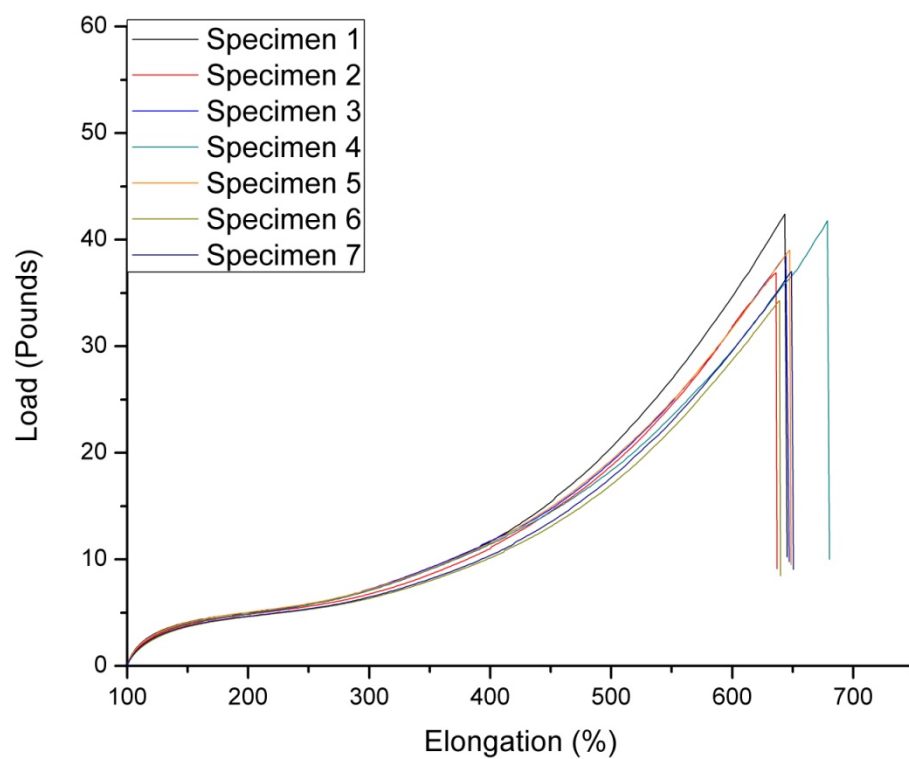


Figure 22. Tensile test results for graphene nanocomposite sample 3.

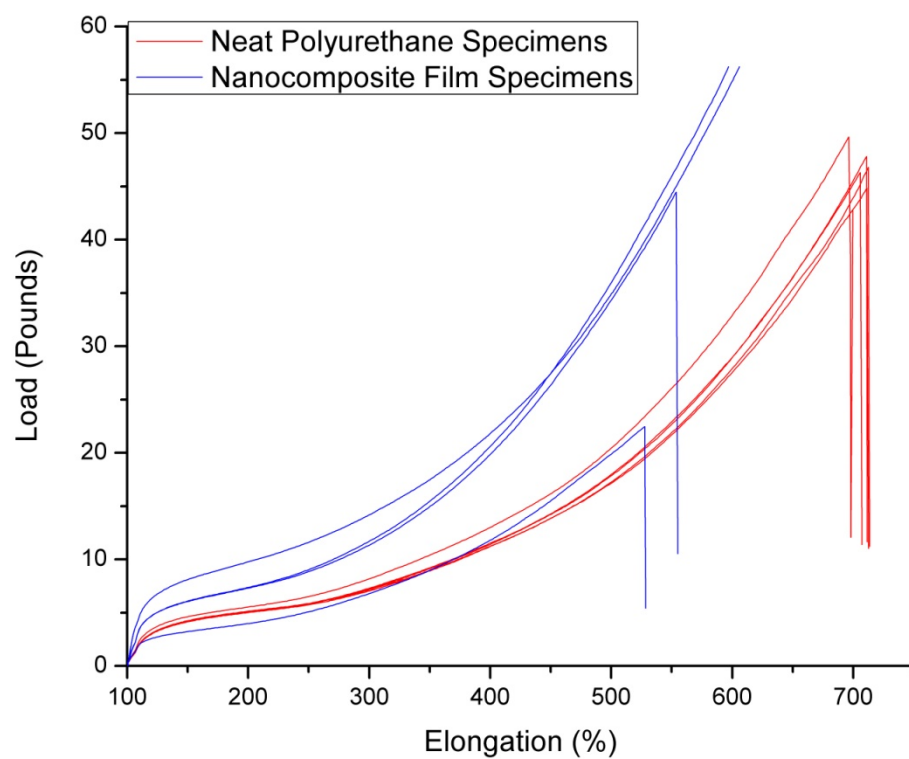


Figure 23. Tensile test results for neat polyurethane and graphene nanocomposite sample 1.

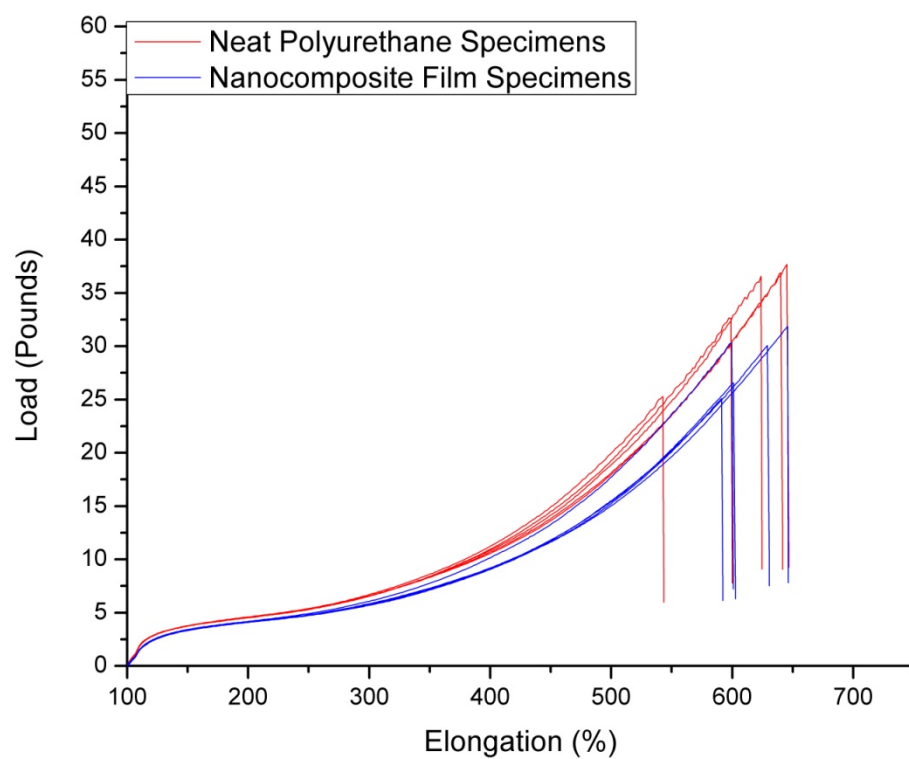


Figure 24. Tensile test results for neat polyurethane and graphene nanocomposite sample 2.

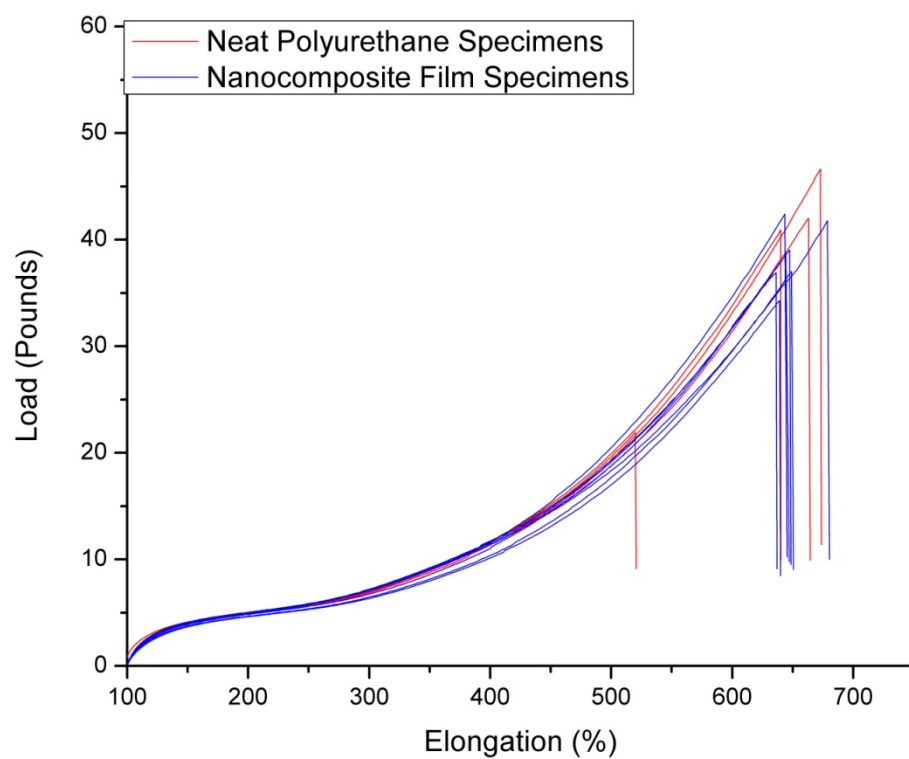


Figure 25. Tensile test results for neat polyurethane and graphene nanocomposite sample 3.

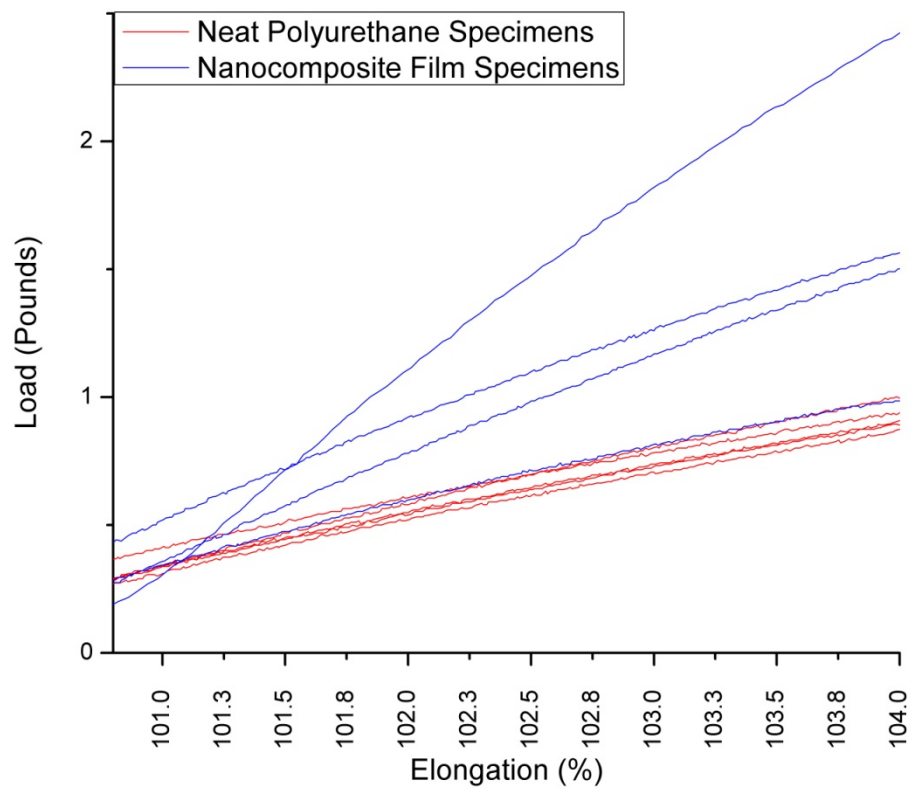


Figure 26. Tensile test results for neat polyurethane and graphene nanocomposite sample 1 showing initial slope.

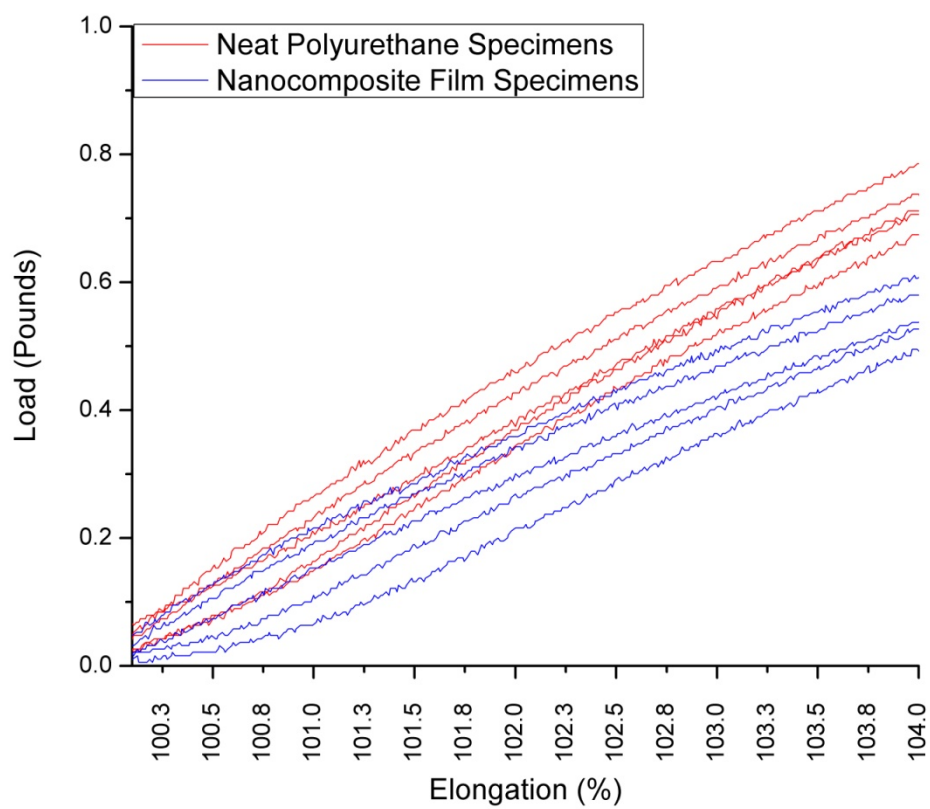


Figure 27. Tensile test results for neat polyurethane and graphene nanocomposite sample 2 showing initial slope.

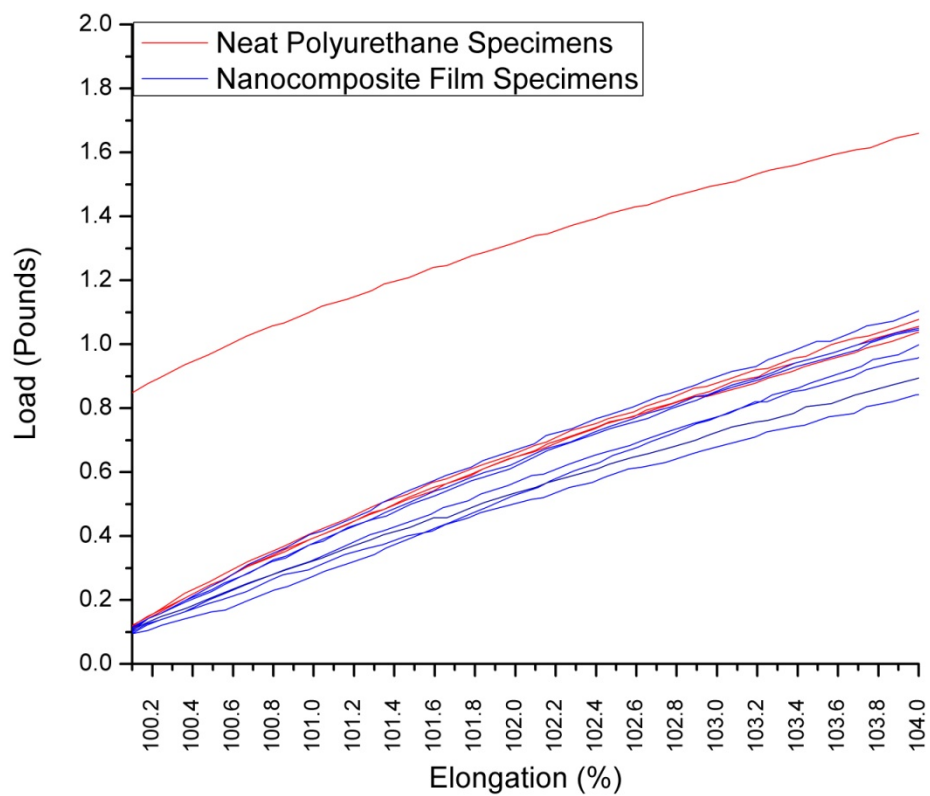


Figure 28. Tensile test results for neat polyurethane and graphene nanocomposite sample 3 showing initial slope.

Table 2. Tensile test results for samples 1-3 neat polyurethane specimens.

Sample Identification	Thickness	Modulus	Peak Load	Average Modulus	Modulus STD DEV	Average Peak Load	Peak Load STD DEV
Neat Polyurethane Sample 1	(Inches)	(PSI)	(Pounds)	(PSI)		(Pounds)	
Specimen 1	0.046	1597.28	46.80	1678.24	194.04	47.06	1.79
Specimen 2	0.045	1602.61	46.30				
Specimen 3	0.043	1722.78	47.80				
Specimen 4	0.047	1479.24	44.80				
Specimen 5	0.043	1989.28	49.60				
Neat Polyurethane Sample 2							
Specimen 1	0.031	2161.41	37.70	2196.29	65.23	33.82	5.14
Specimen 2	0.031	2121.13	36.90				
Specimen 3	0.031	2217.80	36.50				
Specimen 4	0.031	2186.84	25.30				
Specimen 5	0.031	2294.27	32.70				
Neat Polyurethane Sample 3							
Specimen 1	0.058	1441.79	40.90	1453.49	135.22	37.85	10.92
Specimen 2	0.056	1267.16	21.90				
Specimen 3	0.056	1538.51	42.00				
Specimen 4	0.055	1566.49	46.60				

Table 3. Tensile test results for samples 1-3 graphene nanocomposite specimens.

Sample Identification	Thickness	Modulus	Peak Load	Average Modulus	Modulus STD DEV	Average Peak Load	Peak Load STD DEV
Nanocomposite Sample 1	(Inches)	(PSI)	(Pounds)	(PSI)		(Pounds)	
Specimen 1	0.050	5545.05	56.20	4203.87	943.32	44.85	15.89
Specimen 2	0.040	3704.54	56.20				
Specimen 3	0.040	3417.48	44.50				
Specimen 4	0.020	4148.39	22.50				
Nanocomposite Sample 2							
Specimen 1	0.036	1576.55	30.30	1451.92	96.72	28.80	2.83
Specimen 2	0.037	1524.05	26.60				
Specimen 3	0.037	1348.93	25.10				
Specimen 4	0.036	1376.06	30.10				
Specimen 5	0.036	1434.01	31.90				
Nanocomposite Sample 3							
Specimen 1	0.059	1527.27	42.40	1538.65	257.05	38.57	2.85
Specimen 2	0.059	1383.37	36.90				
Specimen 3	0.048	2009.01	38.60				
Specimen 4	0.052	1691.50	41.80				
Specimen 5	0.055	1580.86	39.00				
Specimen 6	0.056	1262.55	34.30				
Specimen 7	0.056	1315.98	37.00				

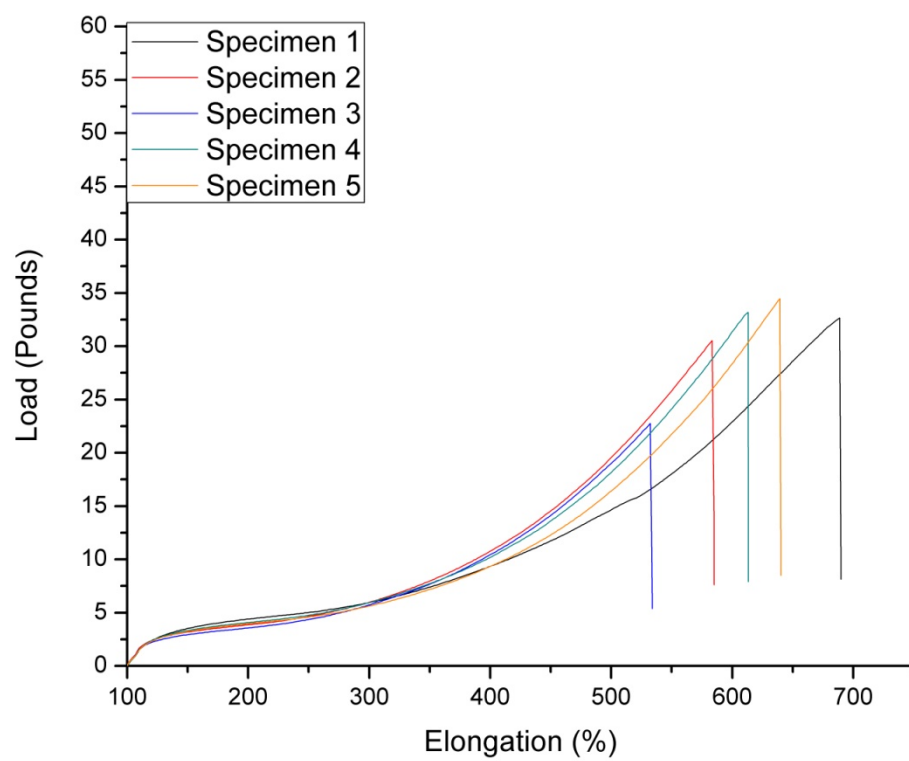


Figure 29. Tensile test results for neat polyurethane sample 4.

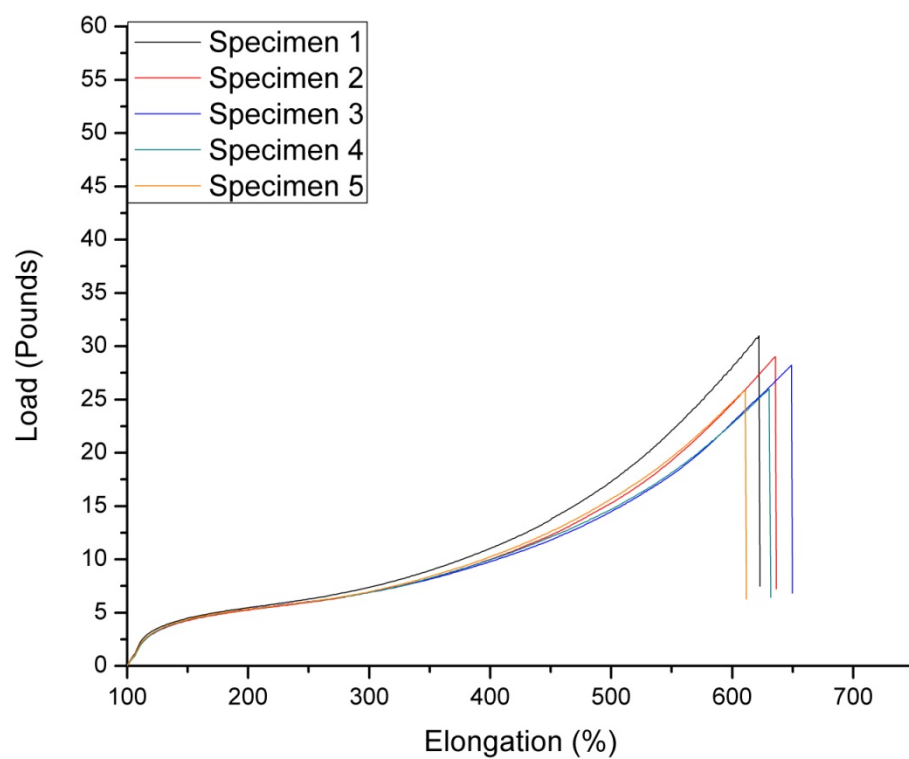


Figure 30. Tensile test results for sodium cloisite nanocomposite film.

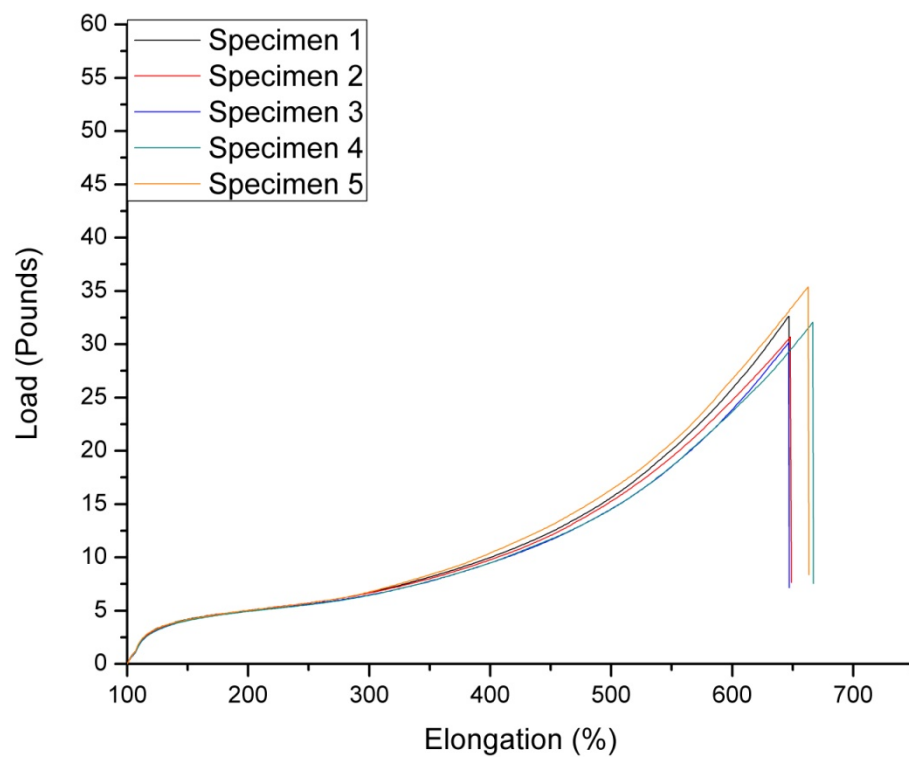


Figure 31. Tensile test results for MWCNT nanocomposite film.

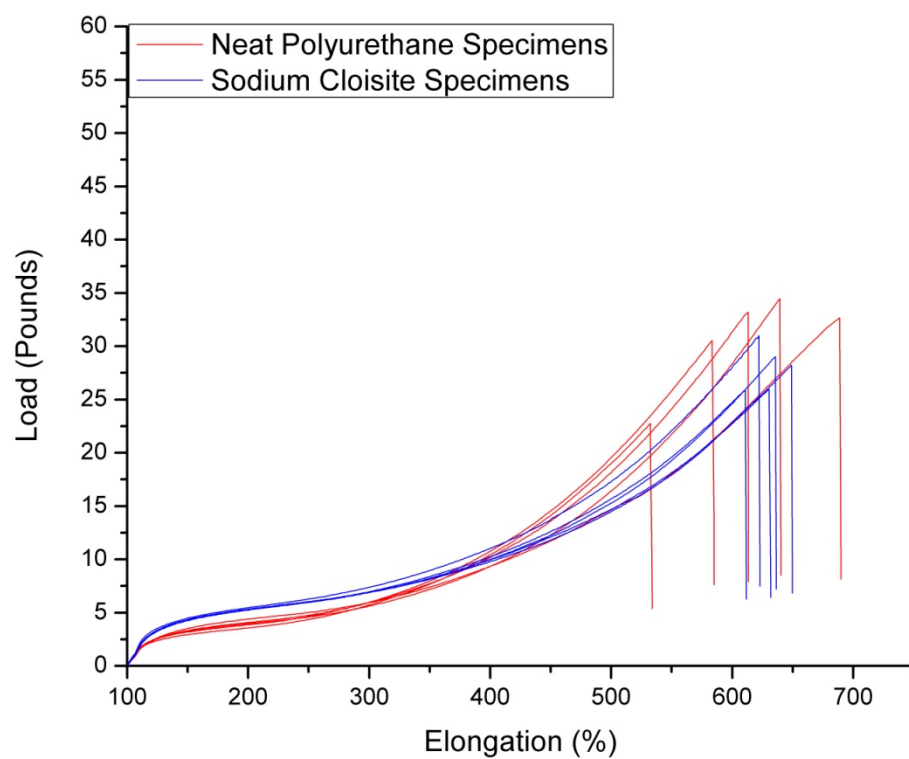


Figure 32. Tensile test results for neat polyurethane sample 4 and the sodium cloisite nanocomposite.

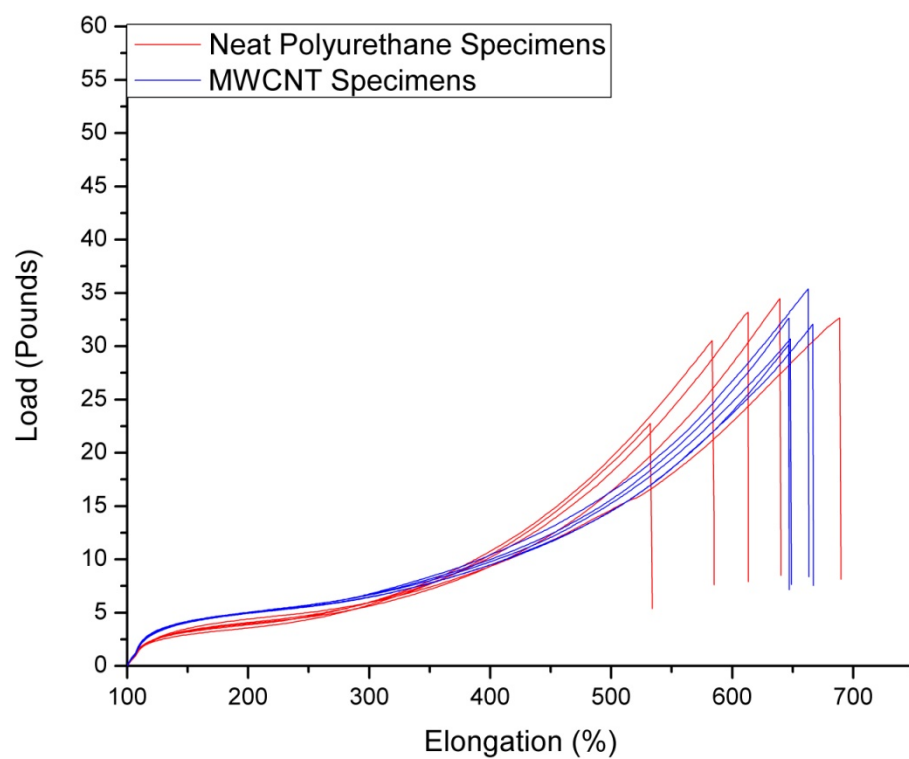


Figure 33. Tensile test results for neat polyurethane sample 4 and the MWCNT nanocomposite.

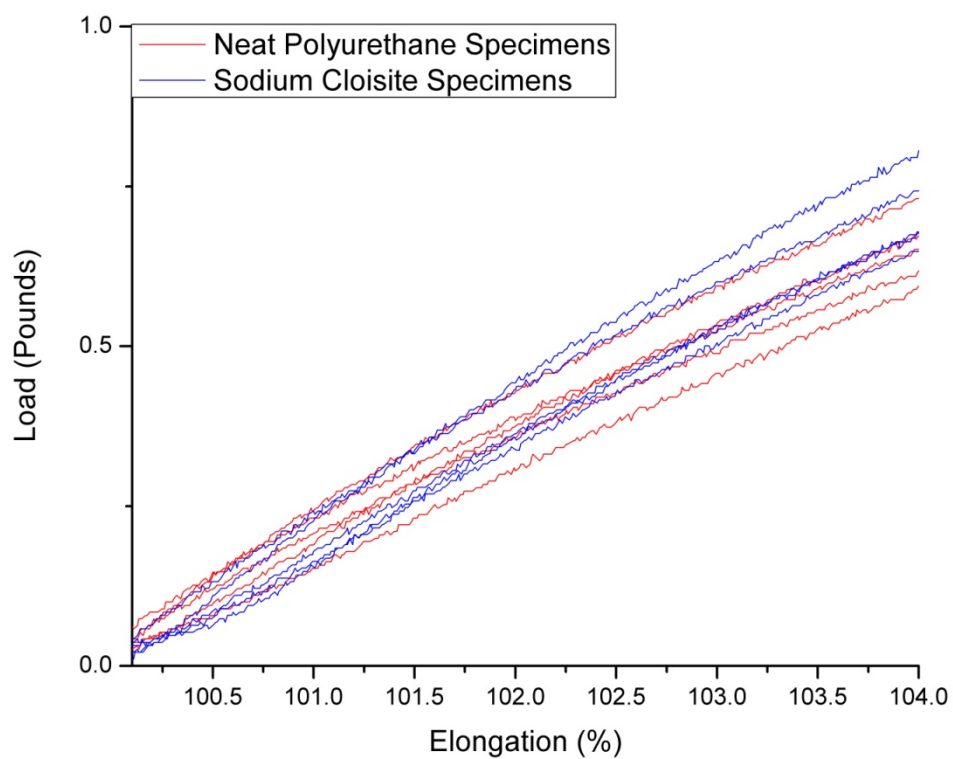


Figure 34. Tensile test results for neat polyurethane sample 4 and the sodium cloisite nanocomposite showing initial slope.

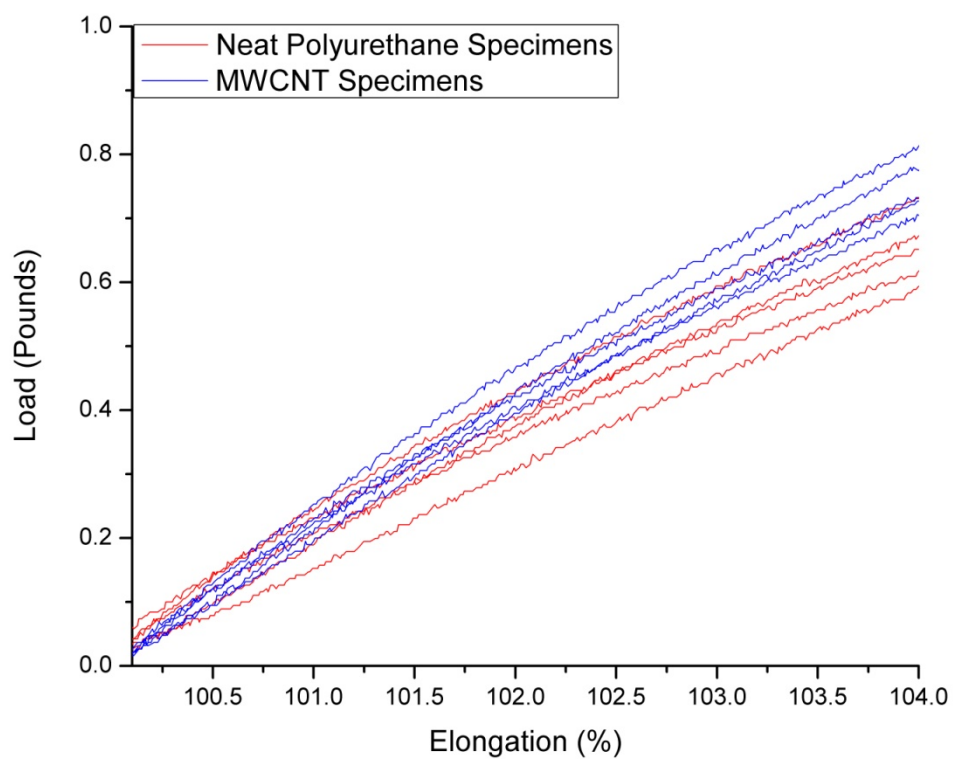


Figure 35. Tensile test results for neat polyurethane sample 4 and MWCNT nanocomposite showing initial slope.

Table 4. Tensile test results for sodium cloisite nanocomposite, MWCNT nanocomposite, and neat polyurethane sample 4 specimens.

Sample Identification	Thickness	Modulus	Peak Load	Average Modulus	Modulus STD DEV	Average Peak Load	Peak Load STD DEV
Sodium Cloisite Nanocomposite	(Inches)	(PSI)	(Pounds)	(PSI)		(Pounds)	
Specimen 1	0.039	1960.10	31.00	1538.43	238.07	28.02	2.15
Specimen 2	0.046	1425.53	29.00				
Specimen 3	0.047	1425.25	28.20				
Specimen 4	0.046	1394.66	26.00				
Specimen 5	0.044	1486.61	25.90				
MWCNT Nanocomposite							
Specimen 1	0.038	1907.99	32.60	1672.52	233.45	32.18	2.07
Specimen 2	0.043	1594.49	30.70				
Specimen 3	0.044	1443.68	30.10				
Specimen 4	0.044	1482.91	32.10				
Specimen 5	0.038	1933.55	35.40				
Neat Polyurethane Sample 4							
Specimen 1	0.038	1410.39	32.60	1436.52	40.70	30.70	4.64
Specimen 2	0.043	1466.34	30.50				
Specimen 3	0.044	1418.65	22.80				
Specimen 4	0.039	1491.75	33.20				
Specimen 5	0.040	1395.49	34.40				

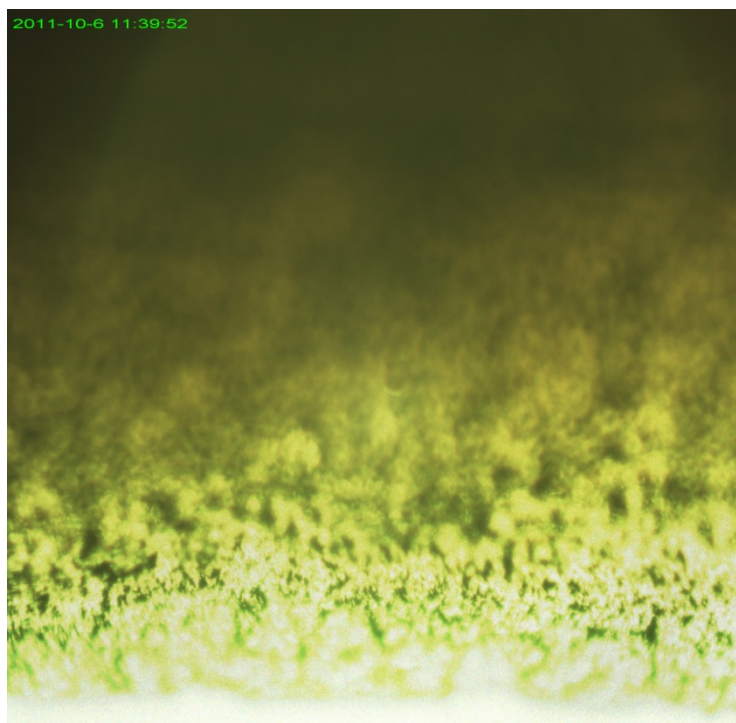


Figure 36. Microscope image for nanocomposite sample 1 (20x objective lens).

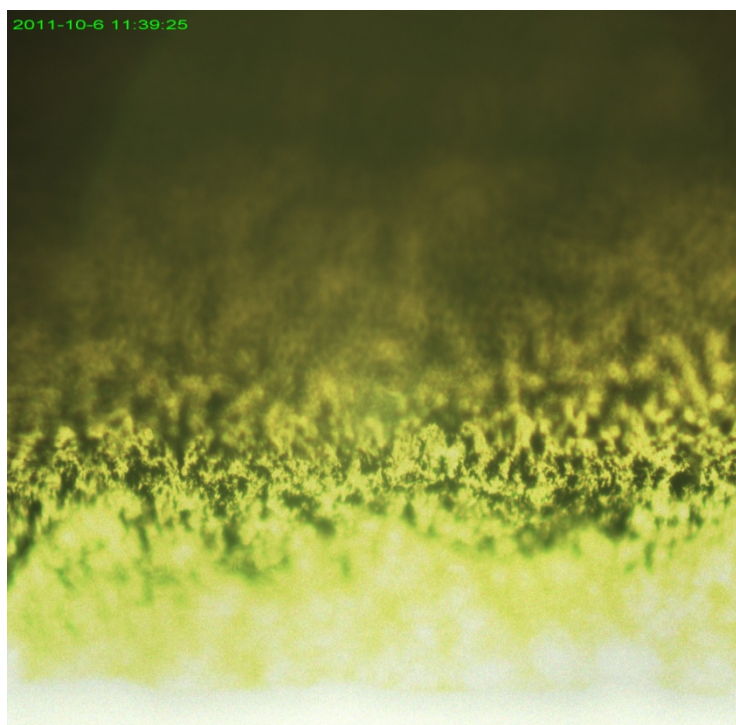


Figure 37. Microscope image for nanocomposite sample 1 (20x objective lens).

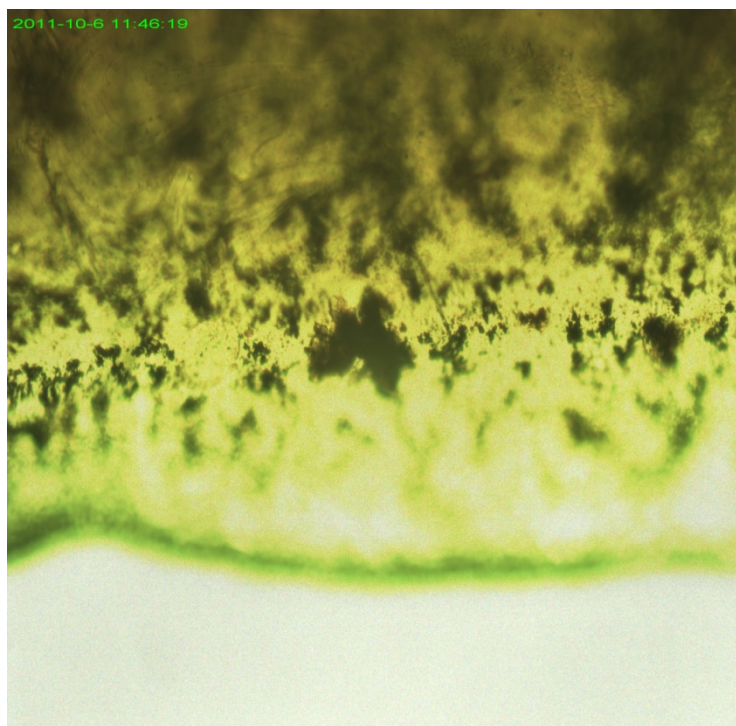


Figure 38. Microscope image for nanocomposite sample 2 (20x objective lens).



Figure 39. Microscope image for nanocomposite sample 2 (20x objective lens).



Figure 40. Microscope image for nanocomposite sample 3 (20x objective lens).

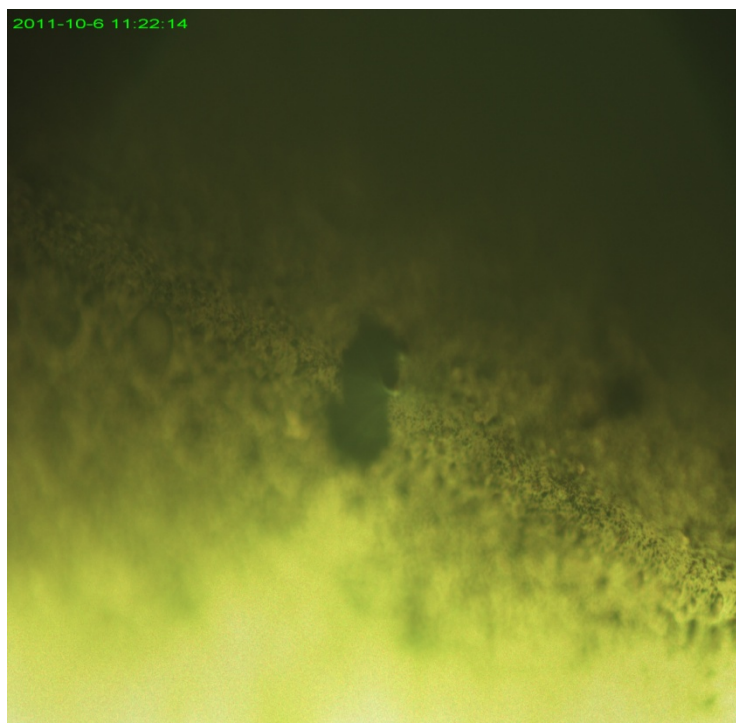


Figure 41. Microscope image for nanocomposite sample 3 (20x objective lens).

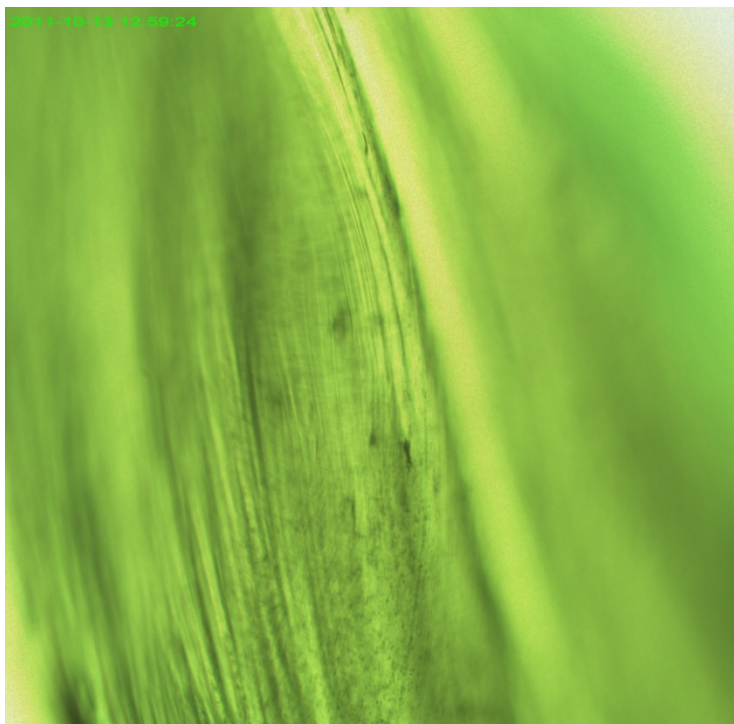


Figure 42. Microscope image for MWCNT nanocomposite film (20x objective lens).

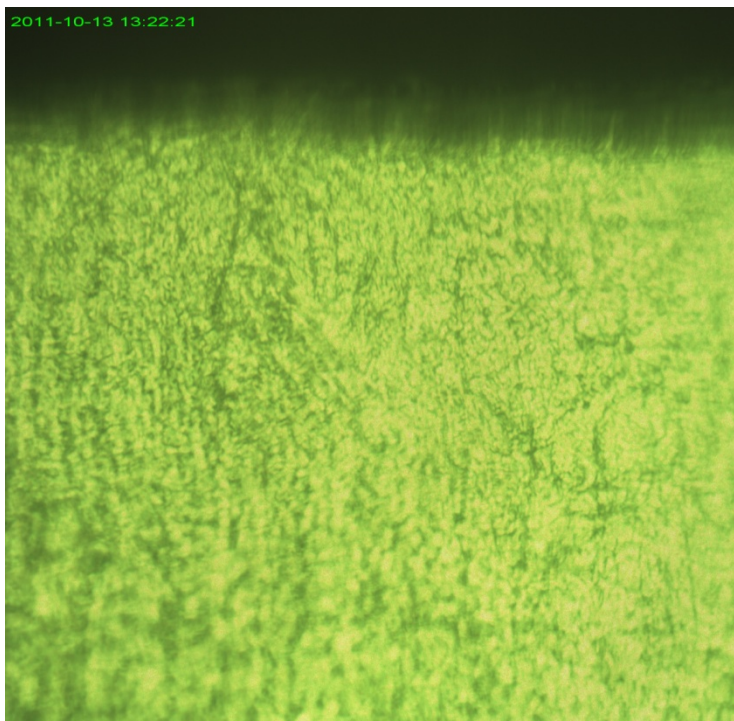


Figure 43. Microscope image for sodium cloisite nanocomposite film (20x objective lens).

4 CONCLUSION AND FUTURE RESEARCH

4.1 Conclusion

The thickness of a graphenol sheet (0.42 nm found in the AFM result) is consistent with the established thickness of a single sheet of graphene of 0.40 nm (6). Although more characterization needs to be done on graphenol sheets regarding the location of the alcohol moieties, and the possibility of other oxygen-containing moieties (e.g. carboxylic acids, epoxides, etc.), this thickness result is encouraging. Aspect ratio was not studied comprehensively but it was found that for graphenol particles identified in the SEM and AFM results aspect ratio ranges from approximately 274:1 to 5952:1.

The tensile test results for the first graphenol nanocomposite film showed over 250% increase of Young's modulus compared to the neat polyurethane film. The tensile test results seem to indicate that upon adequate dispersion, an even higher magnitude of Young's modulus increase may be obtained. It is clear from the second and third samples of graphenol nanocomposite tensile test results that attention must be paid to the level of dispersion of graphenol in this polyurethane matrix. As one might expect, inclusion of graphenol as agglomerates reduces Young's modulus in the nanocomposite and may decrease peak load at break.

4.2 Future Research

Further characterization of graphenol should be undertaken to determine the location of the oxygen atoms in a graphenol sheet. Future characterization should

determine what functional group(s) exist in a graphenol sheet. This would be useful information when determining which matrices are suitable for the inclusion of graphenol in a nanocomposite. A comprehensive investigation into the aspect ratio of graphenol should also be initiated. The polyurethane matrix used in this study had tensile test results that varied between neat samples. It would be useful to choose a matrix in further studies that gives more consistent tensile test results.

Further modification of humic acid or graphenol might prove useful for inclusion in other nanocomposites. This could encompass a host of chemical modifications including any reaction that can be performed on carboxylic acid and alcohol functional groups. Varying degrees of hydrophilicity and hydrophobicity could be designed to facilitate amenable conditions for exfoliation of the nanoparticle in the appropriate matrix. Humic acid and/or graphenol could have polymer linkages which may reduce the likelihood of agglomeration by limiting the mobility of the nanoparticles. This would greatly affect the resulting mechanical properties.

Since these particles appear to be analogues of graphene, both the electrical and thermal conductance of these particles should be evaluated. Nanocomposites including graphenol and its possible products should be evaluated in various matrices at various degrees of loading to determine if there is any desirable modification imposed by this inclusion.

References

- (1) Gupta, R.K.; Kennel, E.; Kim, K.J. *Polymer Nanocomposites Handbook*; CRC Press: Boca Raton, 2010.
- (2) Lee, C.; Wei, X.; Kysar, J.W.; House, J. *Science* **2008**, *321*, 385-8.
- (3) Hu, J.; Ruan, X.; Chen, Y.P. *Nano Lett* **2009**, *9*, 2730-5.
- (4) Heersche, H.B.; Jarillo-Herrero, P.; Oostinga, J.B.; Vandersypen, L.M.K.; Morpurgo, A.F. *Nature* **2007**, *446*, 56-9.
- (5) Rafiee, M.A.; Rafiee, J.; Wang, Z.; Song, H.; Yu, Z.Z.; Koratkar, N. *ACS Nano* **2009**, *3*, 3884-90.
- (6) Novosolev, K.S.; Geim, A.K.; Morozov, S.V.; Jiang, D.; Zhang, Y.; Dubonos, S.V.; et al. *Science* **2004**, *306*, 666-9.
- (7) Stankovich, S.; Dikin, D.A.; Dommett, G.H.B.; Kohlhaas, K.M.; Zimney, E.J.; Stach, E.A.; et al. *Nature* **2006**, *442*, 282-6.
- (8) Viculis, L.M.; Mack, J.J.; Kaner, R.B. *Science* **2003**, *299*, 1361.
- (9) Wang, X.B.; You, H.J.; Liu, F.M.; Li, M.J.; Wan, L.; Li, S.Q.; et al. *Chem Vapor Depos* **2009**, *15*, 53-6.
- (10) Berger, C.; Song, Z.M.; Li, T.B.; Li, X.B.; Ogbazghi, A.Y.; Feng, R.; et al. *J Phys Chem B* **2004**, *108*, 19912-6.
- (11) McAllister, M.J.; Li, J.L.; Adamson, D.H.; Schniepp, H.C.; Abdala, A.A.; Liu, J.; et al. *Chem Mater* **2007**, *19*, 4396-404.

- (12) Leonardite. *Glossary of Geology*, 4th ed.; American Geological Institute: Alexandria, 1997; p 364.
- (13) Tan, K.H. *Humic Matter in Soil and the Environment*; Marcel Dekkar, Inc.: New York, 2003.
- (14) Stevenson, F.J. Geochemistry of Soil Humic Substances. In *Humic Substances in Soil, Sediment, and Water*; Aiken, G.R., McKnight, D.M., Wershaw, R.L., Maccarthy, P., Eds. John Wiley & Sons, Inc.: New York, 1985.
- (15) Dailey, K. Ductile Iron Society.
http://www.ductile.org/magazine/1999_2/leonard.htm (accessed October 12, 2011).
- (16) Silberberg, M.S. *Chemistry: The Molecular Nature of Matter and Change*, 2nd ed.; Mcgraw-Hill: Boston, 2000.
- (17) University of Wisconsin, Department of Chemistry.
<http://chemed.chem.wisc.edu/chempaths/GenChem-Textbook/Conjugated-Systems-1043.html> (accessed on October 12, 2011).
- (18) Hummers, W.S.; Offeman, R.E. *J Am Chem Soc* **1958**, *80*, 1339.
- (19) Beall, G.W. Texas State University-San Marcos, San Marcos, TX. Personal communication, 2011.
- (20) Beall, G.W.; Powell C.E. *Fundamentals of Polymer-Clay Nanocomposites*; Cambridge University Press: Cambridge, 2011.
- (21) Hayakawa, T., Suzuki, T., Uesugi, T., Mitsushima, Y. *Jpn J Appl Phys* **1998**, *37*, 5-9.

VITA

Brandon G. Henderson was born in Santa Rosa, California. He received his high school diploma from Forest Lake Academy, Apopka, Florida. He was awarded an Associate in Arts from South Florida Community College, Avon Park, Florida and a Bachelor of Science from Florida Southern College, Lakeland, Florida. After completing some graduate level courses at University of South Florida, he enlisted in the U. S. Army and served two combat tours with 4th Infantry Division, stationed at Fort Hood, Texas. He entered the Graduate College of Texas State in January, 2010.

Permanent Address: 1013 Chestnut Street
Apt C1
San Marcos, Texas 78666

This thesis was typed by Brandon G. Henderson.